

# Shape monotonicity of the first Steklov–Dirichlet eigenvalue on eccentric annuli <sup>\*</sup>

Jiho Hong<sup>†</sup>

Mikyoung Lim<sup>†</sup>

Dong-Hwi Seo<sup>‡</sup>

## Abstract

In this paper, we investigate the monotonicity of the first Steklov–Dirichlet eigenvalue on eccentric annuli with respect to the distance, namely  $t$ , between the centers of the inner and outer boundaries of annulus. We first show the differentiability of the eigenvalue in  $t$  and obtain an integral expression for the derivative value in two and higher dimensions. We then derive an upper bound of the eigenvalue for each  $t$ , in two dimensions, by the variational formulation. We also obtain a lower bound of the eigenvalue, given a restriction on  $t$  such that the two boundaries of annulus are sufficiently close. The key point of the proof of the lower bound is in analyzing the limit behavior of an infinite series expansion of the first eigenfunction in bipolar coordinates. We also perform numerical experiments that exhibit the monotonicity for two and three dimensions.

**AMS subject classifications.** 35P15, 49R05, 65D99

**Key words.** Steklov eigenvalues; Eigenvalue estimate; Shape derivatives; Bipolar coordinates; Asymptotic analysis

## Contents

<b>1</b>	<b>Introduction</b>	<b>2</b>
<b>2</b>	<b>Variational characterization</b>	<b>6</b>
2.1	Characterization of the first eigenvalue $\sigma_1^t$ on eccentric annuli . . . . .	7
2.2	Upper bound of $\sigma_1^t$ . . . . .	8
<b>3</b>	<b>Differentiability of the first eigenvalue and its shape derivative</b>	<b>8</b>
3.1	Proof of Theorem 1.1 (differentiability of $\sigma_1^t$ and $u_1^t$ ) . . . . .	9
3.2	Proof of Theorem 1.2 (shape derivative of $\sigma_1^t$ ) . . . . .	11

---

<sup>\*</sup>JH and ML are supported by Basic Science Research Program through the National Research Foundation of Korea(NRF) funded by the Ministry of Education(2019R1A6A1A10073887). DS is supported by the National Research Foundation of Korea (NRF) grant number 2017R1D1A1B03036369 funded by the Ministry of Education and grant number 2017R1E1A1A03070543 funded by the Ministry of Science and ICT.

<sup>†</sup>Department of Mathematical Sciences, Korea Advanced Institute of Science and Technology, 291 Daehak-ro, Yuseong-gu, Daejeon 34141, Korea (jihohong@kaist.ac.kr, mklim@kaist.ac.kr).

<sup>‡</sup>Division of Liberal Arts and Sciences, GIST College, Gwangju Institute of Science and Technology, 123 Cheomdangwagi-ro, Buk-gu, Gwangju 61005, Republic of Korea (donghwi.seo26@gmail.com).

<b>4</b>	<b>The first Steklov–Dirichlet eigenfunction in two dimensions in bipolar coordinates</b>	<b>12</b>
4.1	Bipolar coordinates . . . . .	12
4.2	Series expansion of the first eigenfunction . . . . .	14
4.3	Limit behavior of the ratio of consecutive coefficients $\tilde{A}_n$ (i.e., $F_n$ ) . . . . .	16
4.4	Proofs of Lemmas 4.3, 4.4 and Theorem 1.3 . . . . .	17
<b>5</b>	<b>Asymptotic behavior of the first eigenvalue and eigenfunction for small distance between the two boundaries of the annulus</b>	<b>20</b>
5.1	Asymptotic behavior of $T_n$ and $U_n$ . . . . .	20
5.2	Proof of Theorem 1.4 (lower bound of $\sigma_1^t$ ) . . . . .	21
5.3	Asymptotic behavior of $F_n$ . . . . .	22
5.4	Validation of the condition (5.16) in Theorem 5.2 . . . . .	25
<b>6</b>	<b>Numerical computation</b>	<b>26</b>
6.1	Two dimensions . . . . .	27
6.2	Three dimensions . . . . .	32
<b>7</b>	<b>Conclusion</b>	<b>32</b>
	<b>Appendices</b>	<b>34</b>
	<b>Appendix A Proofs of Lemma 6.1 and Proposition 6.2</b>	<b>34</b>
	<b>Appendix B Finite section method in three dimensions</b>	<b>37</b>

# 1 Introduction

We consider the eigenvalue problem for the Laplacian operator on a smooth bounded domain  $\Omega \subset \mathbb{R}^n$  ( $n = 2, 3$ )

$$\Delta u = 0 \quad \text{in } \Omega \tag{1.1}$$

with the Steklov–Dirichlet boundary condition

$$u = 0 \quad \text{on } C_1, \tag{1.2}$$

$$\frac{\partial u}{\partial \nu} = \sigma u \quad \text{on } C_2, \tag{1.3}$$

where  $C_1$  and  $C_2$  are disjoint components of  $\partial\Omega$  and  $\nu$  denotes the unit outward normal vector to  $\partial\Omega$ . If (1.1)–(1.3) admits a non-trivial solution  $u$  for a real constant  $\sigma$ , we call  $u$  an eigenfunction and  $\sigma$  a Steklov–Dirichlet eigenvalue. In this paper, we investigate the spectral geometry of the first (i.e., smallest) nonzero eigenvalue.

A well-studied related problem is the Steklov eigenvalue problem, which is to find  $\sigma \in \mathbb{R}$  for which  $\Delta u = 0$  admits a non-trivial solution satisfying only the Robin boundary condition (1.3). It was proposed by Steklov in 1902 (see [42]); we refer the reader to [28] for the historical background. Another strongly related problem is the Steklov–Neumann problem, which is to find  $\sigma$  for which equations (1.1) and (1.3) admit a non-trivial solution satisfying the zero Neumann condition on  $C_1$ . The Steklov–Dirichlet and its related eigenvalue problems are of importance

from both theoretical and applied perspectives. For example, partially free vibration modes of a thin planar membrane without mass on the interior and with mass on the boundary can be interpreted as Steklov–Dirichlet eigenfunctions [22]; the Steklov–Neumann problem has been studied in relation to hydrodynamics such as the sloshing problem [27]; one can construct the so-called free boundary minimal surfaces in a ball by using the concept of the first Steklov eigenvalue [18, 19, 24, 33, 36]. The Steklov eigenvalue problem is also related to the classical Laplacian eigenvalue problem  $\Delta u = \sigma u$ . For instance, the Steklov eigenvalue can be regarded as limiting Neumann eigenvalues of the Laplacian [8, 30, 31]. It is worth mentioning that the Laplace eigenvalue problems with the Dirichlet, Neumann and Robin boundary conditions have been intensively studied; we refer the reader to the review article [21] and references therein for the properties of the Laplacian eigenvalues and eigenfunctions in various aspects.

Much attention has been focused on the geometric dependence of the first Steklov–Dirichlet eigenvalue in the study of the Steklov–Dirichlet eigenvalue problem. For a planar domain, the upper and lower bounds for the first eigenvalue have been studied by applying the variational approach and the conformal mapping technique [13, 15, 16, 22]. In particular, Hersch and Payne obtained an upper bound for planar annular domains in 1968 [22]. Later, Dittmar and Solynin obtained a lower bound for planar annular domains under some geometric restrictions [16]. We refer the reader to the survey paper by Dittmar [14] for more details. For higher dimensions, Bañuelos et al. obtained a domain monotonicity result and found an inequality relation between the Steklov–Dirichlet and Steklov–Neumann eigenvalues [9]. Recently, Santhanam and Verma considered the Steklov–Dirichlet eigenvalue on eccentric annuli in  $\mathbb{R}^n$ ,  $n > 2$ , with the zero Dirichlet condition on the inner boundary and showed that the first eigenvalue attains the maximum when the annulus is concentric [39]. Seo extended this maximality to some two-point homogeneous spaces including  $\mathbb{R}^2$  [41] (see also the work by Ftouhi [20]).

In the present paper, we investigate the monotonicity of the first Steklov–Dirichlet eigenvalue on eccentric annuli with respect to the distance between the centers of the inner and outer boundaries of annulus. To state our problem and main results more precisely, we introduce some notations. Let  $B_1^t$  and  $B_2$  be the two balls in  $\mathbb{R}^n$  with  $n = 2, 3$  given by

$$B_1^t = B(te_1, r_1), \quad B_2 = B(0, r_2), \quad 0 < r_1 < r_2, \quad 0 \leq t < r_2 - r_1, \quad (1.4)$$

where  $B(x, r)$  denotes the ball centered at  $x \in \mathbb{R}^n$  with radius  $r$ , and  $e_1$  is the unit vector  $(1, 0, \dots, 0) \in \mathbb{R}^n$ . Note that  $\overline{B_1^t} \subset B_2$  for all  $t$  in  $[0, r_2 - r_1)$  and that  $B_1^t$  is concentric with  $B_2$  at  $t = 0$ . We set  $B_1 = B_1^0$ . Figure 1.1 illustrates  $B_1$ ,  $B_1^t$  and  $B_2$ .

We analyze the spectral geometry for the Steklov–Dirichlet eigenvalue problem on the eccentric annulus  $\Omega = B_2 \setminus \overline{B_1^t}$  with zero Dirichlet condition on  $\partial B_1^t$  and Robin condition on  $\partial B_2$ . In other words,

$$\begin{cases} \Delta u^t = 0 & \text{in } B_2 \setminus \overline{B_1^t}, \\ u^t = 0 & \text{on } \partial B_1^t, \\ \frac{\partial u^t}{\partial \nu} = \sigma^t u^t & \text{on } \partial B_2. \end{cases} \quad (1.5)$$

Throughout this paper, we add the superscript  $t$  to  $u$  and  $\sigma$  in order to indicate their dependence on the parameter  $t$ . The spectrum of the Steklov–Dirichlet eigenvalue problem (1.5) is discrete and the sequence of eigenvalues ordered in an ascending order diverges to infinity (see section 2 for details). We denote the first eigenvalue by  $\sigma_1^t$ .

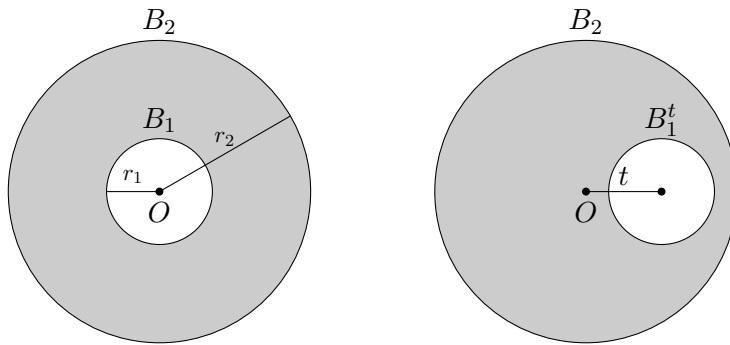


Figure 1.1: Problem geometry: an eccentric annulus  $\Omega = B_2 \setminus \overline{B_1^t}$  (the gray region in the right figure). The two balls are concentric when  $t = 0$ , as in the left figure.

The first eigenvalue  $\sigma_1^t$  attains the maximum at  $t = 0$ , the concentric case, as shown in [20, 39, 41]; the maximal value is  $(r_2(\ln r_2 - \ln r_1))^{-1}$  in two dimensions and  $\frac{r_1}{r_2(r_2 - r_1)}$  in three dimensions. Beyond this, we ask the following:

**Question.** *Is  $\sigma_1^t$  monotone decreasing as  $t$  increases?*

For various Laplacian eigenvalue problems with vanishing boundary condition, the shape monotonicity of the first eigenvalue on eccentric annuli was verified in previous literatures and, in the meantime, similar formulas to (1.6) were derived, for example, by Ramm and Shivakumar [37], Kesavan [25], Aithal and Anisa [2], Anisa and Vemuri [6], Anisa and Mahadevan [5], Anoop et al. [7], and Aithal and Rane [3]. An essential property of the first eigenvalue to prove its monotonicity in the literatures is that the first eigenfunction does not have a sign change in the interior but vanishes on the boundary of annulus. Besides this property, standard techniques for the Laplacian operator, such as the reflection principle and the maximum principle, were used to show that the derivative in  $t$  of the first eigenvalue is negative.

For the eigenvalue problems with the Steklov boundary condition, there have been results which derive an integral formula of the first eigenvalue or verify the maximality at the concentric annulus. In [12], Dambrine et al. obtained an integral formula for the shape derivative of the first eigenvalue of the Wentzell–Laplacian problem, which is a generalization of the Steklov eigenvalue problem. Rodriguez-Quiñones then considered the Steklov eigenvalue problem in two dimensions, based on the result in [12], and showed that the concentric annulus is a critical domain among a class of doubly connected domains [38]. It is then proved by Ftouhi [20] that the first Steklov eigenvalue on eccentric annuli attains the maximum at the concentric case. For the Steklov–Dirichlet eigenvalue problem, as stated previously, the maximality at the concentric annulus was shown by Santhanam and Verma [39], Seo [41], and Ftouhi [20]. However, to the best of our knowledge, the monotonicity is not known either for the Steklov or for the Steklov–Dirichlet eigenvalue problems on eccentric annuli. It is challenging to verify the monotonicity for the eigenvalue with the Steklov boundary condition because the maximum principle technique cannot be applied, differently from the Laplacian eigenvalue problems.

In this paper, first, we show the differentiability of the first eigenvalue and its associated eigenfunction and derive an integral representation for the derivative in  $t$  of the first eigenvalue; see Theorems 1.1, 1.2 below (the proofs are provided in section 3). It is worth remarking that for the Laplacian eigenvalue problem, an integral formula similar to (1.6) was essentially used

to prove the monotonicity of the first eigenvalue.

**Theorem 1.1** (Differentiability). *Let  $B_1^t$  and  $B_2$  be the two eccentric balls in  $\mathbb{R}^n$  ( $n \geq 2$ ) given by (1.4). Let  $\sigma_1^t$  and  $u_1^t$  be the first eigenvalue of the Steklov–Dirichlet eigenvalue problem (1.5) and the corresponding eigenfunction, respectively. Then, the functions*

$$t \mapsto \sigma_1^t \in \mathbb{R} \quad \text{and} \quad t \mapsto u_1^t \in H^1(B_2)$$

*are differentiable with respect to  $t$  in  $[0, r_2 - r_1)$ . Here,  $H^1$  denotes the Sobolev space of order 1.*

**Theorem 1.2** (Shape derivative). *Let  $B_1^t$ ,  $B_2$ ,  $\sigma_1^t$  and  $u_1^t$  be given as in Theorem 1.1. The shape derivative of the first eigenvalue  $\sigma_1^t$  can be expressed as an integral in terms of its associated normalized eigenfunction: for all  $t \in [0, r_2 - r_1)$ ,*

$$\frac{d}{dt} \sigma_1^t = - \int_{\partial B_1^t} \left( \frac{\partial u_1^t}{\partial \nu} \right)^2 (\nu \cdot e_1) dS. \quad (1.6)$$

For further analysis in two dimensions, we employ bipolar coordinates,  $(\xi, \theta) \in \mathbb{R} \times (-\pi, \pi]$ , satisfying that  $\partial B_1^t$  and  $\partial B_2$  are  $\xi$ -level curves of the values, namely,  $\xi_1$  and  $\xi_2$ , respectively (for details, see section 4). The first eigenfunction is naturally expanded into a series of Fourier modes in bipolar coordinates and so is the derivative of the first eigenvalue from the integral formula (1.6). It is then helpful to investigate the behavior of the coefficients of the series expansions to understand the properties of the eigenvalue and eigenfunction. In particular, we deduce the behavior of the ratio of consecutive coefficients in the series expansion of the derivative of the first eigenfunction, namely  $F_n$  (see (4.17) for details), by using the recursive relations among the coefficients, as follows.

**Theorem 1.3.** *For any annulus  $\Omega = B_2 \setminus \overline{B_1^t}$  in two dimensions, there exists a natural number  $n_0$  depending on the shape of  $\Omega$  such that*

$$F_n \leq -e^{-\xi_2} \quad \text{for all } n \geq n_0.$$

The proof of Theorem 1.3 is provided in subsection 4.4. We further investigate the asymptotic behavior of  $F_n$  as  $t \rightarrow (r_2 - r_1)^-$  in subsection 5.3

Dittmar and Solynin obtained a lower bound of the first Steklov–Dirichlet eigenvalue on a ring domains in two dimensions [16]. In the following theorem, by using Theorem 1.3, we derive a lower bound for the liminf of the first eigenvalue, which provides a finer estimate given some conditions on  $r_1, r_2$  and  $t$ ; see Remark 1 in subsection 5.2 for details. The proof of Theorem 1.4 is provided in subsection 5.2.

**Theorem 1.4** (Lower bound in two dimensions). *Let  $\sigma_1^t$  be the first Steklov–Dirichlet eigenvalue of  $\Omega = B_2 \setminus \overline{B_1^t}$  in two dimensions. It holds that*

$$\liminf_{t \rightarrow (r_2 - r_1)^-} \sigma_1^t \geq \frac{r_1}{2r_2(r_2 - r_1)}. \quad (1.7)$$

In addition to analytical results, we perform numerical computation for the first Steklov–Dirichlet eigenvalue on eccentric annuli in two and three dimensions by using bipolar and bi-spherical coordinates, respectively. Numerical results show that  $\sigma_1^t$  is monotone decreasing as  $t$  increases.

The remainder of this paper is organized as follows. In section 2, we provide the variational characterization for the first Steklov–Dirichlet eigenvalue. Section 3 is devoted to deriving the integral formula for the shape derivative of the first eigenvalue, after showing its differentiability. In section 4, we introduce bipolar coordinates for planar domains and obtain series expansions for the first eigenvalue and eigenfunction. We then investigate analytic properties of the first eigenvalue and eigenfunction in section 5. In section 6, we provide numerical evidence for the monotonicity of the first eigenvalue for both two and three dimensions. We finish with the conclusion in section 7.

## 2 Variational characterization

We first explain the variational characterization of the first Steklov–Dirichlet eigenvalue for a domain in a Riemannian manifold. Let  $M^n$  be a Riemannian manifold of dimension  $n \geq 2$  and  $\Omega \subset M$  a bounded domain with smooth boundary  $\partial\Omega$ . Let  $\partial\Omega = C_1 \cup C_2$ , where  $C_1$  and  $C_2$  are disjoint components of  $\partial\Omega$ . The Steklov–Dirichlet eigenvalue problem on  $\Omega$  is to find  $\sigma \in \mathbb{R}$  for which there exists a non-trivial solution  $u \in C^\infty(M)$  satisfying

$$\begin{cases} \Delta u = 0 & \text{in } \Omega, \\ u = 0 & \text{on } C_1, \\ \frac{\partial u}{\partial \nu} = \sigma u & \text{on } C_2, \end{cases} \quad (2.1)$$

where  $\nu$  is the outward unit normal vector along  $C_2$ . When  $C_1 = \emptyset$  and  $C_2$  is connected, (2.1) becomes the classical Steklov eigenvalue problem (see [42]).

The Steklov–Dirichlet eigenvalue problem (2.1) is equivalent to the eigenvalue problem of the Dirichlet-to-Neumann operator

$$\begin{aligned} L : C^\infty(C_2) &\longrightarrow C^\infty(C_2) \\ \hat{u} &\longmapsto \left. \frac{\partial u}{\partial \nu} \right|_{C_2}, \end{aligned} \quad (2.2)$$

where  $u$  is the extension of  $\hat{u}$  satisfying

$$\begin{cases} \Delta u = 0 & \text{in } \Omega, \\ u = 0 & \text{on } C_1, \\ u = \hat{u} & \text{on } C_2. \end{cases}$$

The operator  $L$  is positive-definite, self-adjoint with respect to the  $L^2$  inner-product and has a discrete spectrum (see, for example, [1])

$$0 < \sigma_1(\Omega) \leq \sigma_2(\Omega) \leq \dots \rightarrow \infty,$$

provided that  $C_1 \neq \emptyset$ . We call  $\sigma_k(\Omega)$  the  $k$ th (Steklov–Dirichlet) eigenvalue. We call the corresponding  $\hat{u}$  and its harmonic extension  $u$  the  $k$ th eigenfunction.

The first eigenvalue  $\sigma_1(\Omega)$  admits the variational characterization (see, for example, [10]):

$$\sigma_1(\Omega) = \inf \left\{ \frac{\int_{\Omega} |\nabla v|^2 dx}{\int_{C_2} v^2 dS} \mid v \in H^1(\Omega) \setminus \{0\} \text{ and } v = 0 \text{ on } C_1 \right\}. \quad (2.3)$$

## 2.1 Characterization of the first eigenvalue $\sigma_1^t$ on eccentric annuli

We now go back to the problem (1.5). We remind that

$$\sigma_1^t = \sigma_1(B_2 \setminus \overline{B_1^t})$$

with  $C_1 = \partial B_1^t$  and  $C_2 = \partial B_2$ . It admits the normalized eigenfunction  $u_1^t \in H^1(B_2 \setminus \overline{B_1^t})$  satisfying

$$u_1^t \geq 0 \quad \text{in } B_2 \setminus \overline{B_1^t}, \quad (2.4)$$

$$\int_{\partial B_2} (u_1^t)^2 dS = 1. \quad (2.5)$$

The positiveness (2.4) is supported by the following lemma.

**Lemma 2.1.** *The first eigenfunction  $u_1^t$  does not change the sign in  $B_2 \setminus \overline{B_1^t}$ . Furthermore,  $\sigma_1^t$  is simple.*

*Proof.* Suppose  $u_1^t$  has both positive and negative values. Let  $(u_1^t)^+ = \max(u_1^t, 0)$  and  $(u_1^t)^- = \max(-u_1^t, 0)$ . Then, from the smoothness of  $u_1^t$ , we have  $(u_1^t)^+, (u_1^t)^- \in H^1(\Omega) \setminus \{0\}$  and

$$\begin{aligned} \int_{B_2 \setminus \overline{B_1^t}} |\nabla u_1^t|^2 dx &= \int_{B_2 \setminus \overline{B_1^t}} |\nabla (u_1^t)^+|^2 dx + \int_{B_2 \setminus \overline{B_1^t}} |\nabla (u_1^t)^-|^2 dx, \\ \int_{\partial B_2} (u_1^t)^2 dS &= \int_{\partial B_2} ((u_1^t)^+)^2 dS + \int_{\partial B_2} ((u_1^t)^-)^2 dS. \end{aligned}$$

Since  $u_1^t$  is the first eigenfunction, the variational characterization (2.3) implies

$$\sigma_1^t = \frac{\int_{B_2 \setminus \overline{B_1^t}} |\nabla u_1^t|^2 dx}{\int_{\partial B_2} (u_1^t)^2 dS} \geq \min \left( \frac{\int_{B_2 \setminus \overline{B_1^t}} |\nabla (u_1^t)^+|^2 dx}{\int_{\partial B_2} ((u_1^t)^+)^2 dS}, \frac{\int_{B_2 \setminus \overline{B_1^t}} |\nabla (u_1^t)^-|^2 dx}{\int_{\partial B_2} ((u_1^t)^-)^2 dS} \right) \geq \sigma_1^t.$$

Therefore,  $(u_1^t)^+$  or  $(u_1^t)^-$  is also the first eigenfunction from the variational characterization (2.3) and, thus, satisfies (1.5). Both  $(u_1^t)^+$  and  $(u_1^t)^-$  are positive in some open subset of  $B_2 \setminus \overline{B_1^t}$  from the assumption on  $u_1^t$  and, consequently, they are zero in some open subset. It contradicts, in view of the maximum principle, that  $(u_1^t)^+$  or  $(u_1^t)^-$  satisfies (1.5). Therefore the first eigenfunction  $u_1^t$  is not sign-changing. Then a function orthogonal to  $u_1^t$  is sign-changing, so it cannot be the first eigenfunction. It implies  $\sigma_1^t$  is simple.  $\square$

We can identify the two function spaces

$$\left\{ u \in H^1(B_2 \setminus \overline{B_1^t}) \mid u = 0 \text{ on } \partial B_1^t \right\} \quad \text{and} \quad H_{\overline{B_1^t}}^1(B_2), \quad (2.6)$$

where

$$H_A^1(\Omega) := \{ u \in H^1(\Omega) \mid u = 0 \text{ in } A \}$$

for a subset  $A \subset \overline{\Omega}$ . Hence, we can regard  $u_1^t$  as a function in  $H_{\overline{B_1^t}}^1(B_2) \subset H^1(B_2)$  and  $\sigma_1^t$  also admits the following variational characterization:

$$\sigma_1^t = \inf \left\{ \frac{\int_{B_2} |\nabla v|^2 dx}{\int_{\partial B_2} v^2 dS} \mid v \in H_{\overline{B_1^t}}^1(B_2) \setminus \{0\} \right\}. \quad (2.7)$$

## 2.2 Upper bound of $\sigma_1^t$

We obtain an upper bound of the first eigenvalue by using the variational formulation.

**Theorem 2.2** (Upper bound in two dimensions). *Let  $B_1^t$  and  $B_2$  be the two eccentric balls in  $\mathbb{R}^2$  given by (1.4). For any  $t \in [0, r_2 - r_1)$ , it holds that*

$$\sigma_1^t \leq \frac{\pi(r_2^2 - r_1^2)}{2\pi r_2(r_2^2 + r_1^2 + t^2) - 4r_1 r_2 \int_0^\pi \sqrt{r_2^2 - 2r_2 t \cos \varphi + t^2} d\varphi}. \quad (2.8)$$

*Proof.* We take a test function  $v$  as

$$v(x) = |x - (t, 0)| - r_1. \quad (2.9)$$

As  $B_1^t$  is centered at  $(t, 0)$  with radius  $r_1$ ,  $v$  is zero on  $\partial B_1^t$ . Figure 2.1 compares the level curves of  $v$  and the first eigenfunction. We have

$$\int_{B_2 \setminus \overline{B_1^t}} |\nabla v|^2 dx = \int_{B_2 \setminus \overline{B_1^t}} 1 dx = \pi(r_2^2 - r_1^2). \quad (2.10)$$

By parameterizing  $\partial B_2$  as  $(r_2 \cos \varphi, r_2 \sin \varphi)$ ,  $-\pi \leq \varphi < \pi$ , it follows that

$$v|_{\partial B_2} = \sqrt{r_2^2 - 2r_2 t \cos \varphi + t^2} - r_1$$

and

$$\int_{\partial B_2} v^2 dS = 2\pi r_2(r_2^2 + r_1^2 + t^2) - 4r_1 r_2 \int_0^\pi \sqrt{r_2^2 - 2r_2 t \cos \varphi + t^2} d\varphi.$$

From (2.7), we prove the theorem. □

Since the integrand  $\sqrt{r_2^2 - 2r_2 t \cos \varphi + t^2}$  in (2.8) is monotone increasing in  $\varphi$ , we have for any  $N \in \mathbb{N}$ ,

$$\int_0^\pi \sqrt{r_2^2 - 2r_2 t \cos \varphi + t^2} d\varphi \leq \frac{\pi}{N} \sum_{n=1}^N \sqrt{r_2^2 - 2r_2 t \cos \frac{n\pi}{N} + t^2}.$$

In particular, by letting  $N = 100$  and applying Theorem 2.2, we obtain

$$\sigma_1^t \leq M(t) := \frac{\pi(r_2^2 - r_1^2)}{2\pi r_2(r_2^2 + r_1^2 + t^2) - 4r_1 r_2 \frac{\pi}{100} \sum_{n=1}^{100} \sqrt{r_2^2 - 2r_2 t \cos \frac{n\pi}{100} + t^2}}. \quad (2.11)$$

We will use this upper bound later in subsection 5.4.

## 3 Differentiability of the first eigenvalue and its shape derivative

In this section, we prove Theorems 1.1, 1.2 by using the variational characterization.

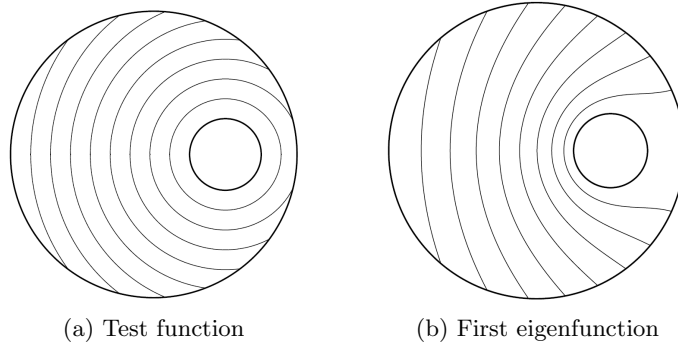


Figure 2.1: Level curves of the test function given in (2.9) and the numerically computed first eigenfunction for an eccentric annulus with  $r_1 = 1, r_2 = 4, t = 2$ .

### 3.1 Proof of Theorem 1.1 (differentiability of $\sigma_1^t$ and $u_1^t$ )

The outline of the proof follows an argument of [17].

For  $t_0 \in [0, r_2 - r_1)$  and  $s > 0$  satisfying  $t_0 + s < r_2 - r_1$ , we consider the first eigenfunction  $\sigma_1^{t_0+s}$  and its associated normalized eigenfunction  $u_1^{t_0+s}$  of the eigenvalue problem (1.5) (see also (2.4) and (2.5)). Then, the following weak formulation holds using the function spaces identification (2.6):

$$\int_{B_2} \nabla u_1^{t_0+s} \cdot \nabla \varphi \, dx = \sigma_1^{t_0+s} \int_{\partial B_2} u_1^{t_0+s} \varphi \, dS \quad \text{for all } \varphi \in H_{\overline{B_1^{t_0+s}}}^1(B_2). \quad (3.1)$$

Let  $V : \overline{B_2} \rightarrow \mathbb{R}^n$  be a variation field on  $\overline{B_2}$  generated by the moving of  $B_1^{t_0}$  to  $e_1$ -direction fixing  $\partial B_2$ . In particular,  $V$  is a smooth vector field satisfying

$$V = e_1 \text{ on } \overline{B_1^{t_0}} \quad \text{and} \quad \text{supp}(V) \subset B_2.$$

We now define a map  $\Phi : (-r_2 + r_1 - t_0, r_2 - r_1 - t_0) \times B_2 \rightarrow \mathbb{R}^n$  by

$$\Phi(s, x) = x + sV(x).$$

Clearly, it holds that  $\Phi(s, B_2) = B_2$  and  $u_1^{t_0+s} \circ \Phi(s, \cdot) \in H_{\overline{B_1^{t_0}}}^1$ . Since

$$D\Phi(0, \cdot) = Id, \quad (3.2)$$

there is a neighborhood  $U_1$  of 0 in  $\mathbb{R}$  such that  $\Phi(s, \cdot)$  is a diffeomorphism of  $B_2$ . By the change of variables formula and the chain rule, (3.1) becomes

$$\begin{aligned} & \int_{B_2} \left( \nabla (u_1^{t_0+s} \circ \Phi(s, \cdot)) (D\Phi(s, \cdot))^{-1} \right) \cdot \left( \nabla (\varphi \circ \Phi(s, \cdot)) (D\Phi(s, \cdot))^{-1} \right) |D\Phi(s, \cdot)| \, dx \\ &= \sigma_1^{t_0+s} \int_{\partial B_2} (u_1^{t_0+s} \circ \Phi(s, \cdot)) (\varphi \circ \Phi(s, \cdot)) \, dS, \end{aligned} \quad (3.3)$$

and (2.5) becomes

$$\int_{\partial B_2} (u_1^{t_0+s} \circ \Phi(s, \cdot))^2 \, dS = 1. \quad (3.4)$$

We denote  $(H_{\bar{B}_1}^1(B_2))'$  the dual space of  $H_{\bar{B}_1}^1(B_2)$  and  $\langle \cdot, \cdot \rangle$  the dual pairing between  $(H_{\bar{B}_1}^1(B_2))'$  and  $H_{\bar{B}_1}^1(B_2)$ . We then define

$$f = (f_1, f_2) : U_1 \times H_{\bar{B}_1}^1(B_2) \times \mathbb{R} \rightarrow (H_{\bar{B}_1}^1(B_2))' \times \mathbb{R}$$

by

$$\begin{cases} \langle f_1(s, v, \sigma), \psi \rangle &= \int_{B_2} ((\nabla v)(D\Phi(s, \cdot))^{-1}) \cdot ((\nabla \psi)(D\Phi(s, \cdot))^{-1}) |D\Phi(s, \cdot)| dx - \sigma \int_{\partial B_2} v\psi dS, \\ f_2(s, v, \sigma) &= \int_{\partial B_2} v^2 dS - 1 \end{cases}$$

for all  $\psi \in H_{\bar{B}_1}^1(B_2)$ . Clearly,  $f$  is  $C^1$  near  $(0, u_1^{t_0}, \sigma_1^{t_0})$ . In addition, we set

$$\begin{aligned} g : U_1 &\rightarrow H_{\bar{B}_1}^1(B_2) \times \mathbb{R} \\ s &\mapsto (u_1^{t_0+s} \circ \Phi(s, \cdot), \sigma_1^{t_0+s}). \end{aligned}$$

Then, equations (3.3) and (3.4) imply

$$f(s, g(s)) = 0 \quad \text{for all } s \in U_1.$$

If we show

$$\frac{\partial f}{\partial(v, \sigma)} \Big|_{(0, u_1^{t_0}, \sigma_1^{t_0})} : H_{\bar{B}_1}^1(B_2) \times \mathbb{R} \longrightarrow (H_{\bar{B}_1}^1(B_2))' \times \mathbb{R} \quad (3.5)$$

is an isomorphism, then  $g$  is  $C^1$  by the implicit function theorem (see, for instance, [43, Theorem 4.B]) and Theorem 1.1 is proved.

In the remaining of the proof, we show that (3.5) is an isomorphism. That is, for any  $(h, \lambda) \in (H_{\bar{B}_1}^1(B_2))' \times \mathbb{R}$ , we will find a unique element  $(w, \mu) \in H_{\bar{B}_1}^1(B_2) \times \mathbb{R}$  such that

$$\langle h, \psi \rangle = \left\langle \frac{\partial f_1}{\partial(v, \sigma)} \Big|_{(0, u_1^{t_0}, \sigma_1^{t_0})} (w, \mu), \psi \right\rangle \quad \text{for all } \psi \in H_{\bar{B}_1}^1(B_2), \quad (3.6)$$

$$\lambda = \frac{\partial f_2}{\partial(v, \sigma)} \Big|_{(0, u_1^{t_0}, \sigma_1^{t_0})} (w, \mu), \quad (3.7)$$

where, from (3.2) and the definition of  $f$ , the right-hand sides are

$$\left\langle \frac{\partial f_1}{\partial(v, \sigma)} \Big|_{(0, u_1^{t_0}, \sigma_1^{t_0})} (w, \mu), \psi \right\rangle = \int_{B_2} \nabla w \cdot \nabla \psi dx - \int_{\partial B_2} (\sigma_1^{t_0} w + \mu u_1^{t_0}) \psi dS, \quad (3.8)$$

$$\frac{\partial f_2}{\partial(v, \sigma)} \Big|_{(0, u_1^{t_0}, \sigma_1^{t_0})} (w, \mu) = 2 \int_{\partial B_2} u_1^{t_0} w dS. \quad (3.9)$$

We define two linear maps  $S_1, S_2 : H_{\bar{B}_1}^1(B_2) \longrightarrow (H_{\bar{B}_1}^1(B_2))'$  by

$$\begin{aligned} \langle S_1(v), \psi \rangle &= \int_{\partial B_2} v\psi dS, \\ \langle S_2(v), \psi \rangle &= \int_{B_2} v\psi dx \quad \text{for } v, \psi \in H_{\bar{B}_1}^1(B_2). \end{aligned}$$

In fact,  $S_1$  is the composition of the following three mappings:

$$H_{\bar{B}_1^{t_0}}^1(B_2) \subset\subset L^2(\partial B_2) \xrightarrow{\text{isometry}} (L^2(\partial B_2))' \subset\subset (H_{\bar{B}_1^{t_0}}^1(B_2))',$$

where  $(L^2(\partial B_2))'$  is the dual space of  $L^2(\partial B_2)$ . The first inclusion is compact from the compact embedding  $H^1(B_2) \subset\subset L^2(\partial B_2)$  (see, e.g., [29, Theorem 2.31, 2.33] or [35, Theorem 1.2 in Chapter 1]). Furthermore, the Schauder theorem (see, e.g., [11, Theorem 6.4]) implies that the third map is compact and, thus,  $S_1$  is compact. Similarly,  $S_2$  is compact.

Now, we go back to equation (3.6), which, in view of (3.8), can be rewritten as

$$\langle h, \psi \rangle = (w, \psi) - \langle (\sigma_1^{t_0} S_1 + S_2)(w), \psi \rangle - \langle \mu S_1(u_1^{t_0}), \psi \rangle,$$

where  $(w, \psi)$  is the inner product in  $H_{\bar{B}_1^{t_0}}^1(B_2)$ . In other words,

$$(w, \psi) - \langle (\sigma_1^{t_0} S_1 + S_2)(w), \psi \rangle = \langle h, \psi \rangle + \langle \mu S_1(u_1^{t_0}), \psi \rangle. \quad (3.10)$$

We can regard  $h$ ,  $(\sigma_1^{t_0} S_1 + S_2)(w)$  and  $S_1(u_1^{t_0})$ , that are elements in the dual space of  $H_{\bar{B}_1^{t_0}}^1(B_2)$ , as functions in  $H_{\bar{B}_1^{t_0}}^1(B_2)$ . Since  $\sigma_1^{t_0} S_1 + S_2$  is compact and self-adjoint, there is a unique solution  $w$  to (3.10) up to kernel  $(Id - (\sigma_1^{t_0} S_1 + S_2)) = \text{span}(u_1^{t_0})$  if and only if

$$h + \mu S_1(u_1^{t_0}) \perp u_1^{t_0}, \quad (3.11)$$

by the Fredholm alternative (see, e.g., [40, Corollary 8.1]). Because of  $\langle S_1(u_1^{t_0}), u_1^{t_0} \rangle \neq 0$ , we can uniquely find  $\mu$  satisfying (3.11). Furthermore, equation (3.10) with (3.7) and (3.9) uniquely determine  $w$ . Therefore, (3.5) is an isomorphism and it finishes the proof.  $\square$

In the following subsection, we calculate the derivative of  $\sigma_1^t$  with respect to  $t$ .

### 3.2 Proof of Theorem 1.2 (shape derivative of $\sigma_1^t$ )

We use the same notation of  $V, \Phi$  as in the proof of Theorem 1.1.

For  $x \in \partial B_1^{t_0}$ , we have

$$\begin{aligned} 0 &= \frac{d}{ds} \Big|_{s=0} (u^{t_0+s}(\Phi(s, x))) = (u_1^{t_0})'(x) + (\nabla u_1^{t_0} \cdot e_1) \\ &= (u_1^{t_0})'(x) + \frac{\partial u_1^{t_0}}{\partial \nu^{t_0}} (\nu^{t_0} \cdot e_1). \end{aligned}$$

Hence, it follows that

$$\begin{cases} \Delta(u_1^{t_0})' = 0 & \text{in } B_2 \setminus \overline{B_1^{t_0}} \\ (u_1^{t_0})' = -\frac{\partial u_1^{t_0}}{\partial \nu^{t_0}} (\nu^{t_0} \cdot e_1) & \text{on } \partial B_1^{t_0} \end{cases}$$

We then obtain by using the Robin boundary condition on  $\partial B_2$  and (2.5) that

$$\begin{aligned} \int_{\partial(B_2 \setminus \overline{B_1^{t_0}})} \frac{\partial u_1^{t_0}}{\partial \nu^{t_0}} (u_1^{t_0})' dS &= \int_{\partial B_1^{t_0}} \frac{\partial u_1^{t_0}}{\partial \nu^{t_0}} (u_1^{t_0})' dS + \sigma_1^{t_0} \int_{\partial B_2} u_1^{t_0} (u_1^{t_0})' dS \\ &= - \int_{\partial B_1^{t_0}} \left( \frac{\partial u_1^{t_0}}{\partial \nu^{t_0}} \right)^2 (\nu^{t_0} \cdot e_1) dS. \end{aligned} \quad (3.12)$$

On the other hand, for  $y \in \partial B_2$ , we have

$$\frac{\partial u_1^{t_0+s}}{\partial \nu}(y) = \sigma_1^{t_0+s} u_1^{t_0+s}(y) \quad \text{and} \quad \Phi(s, y) = y,$$

which implies

$$\frac{\partial(u_1^{t_0})'}{\partial \nu}(y) = (\sigma_1^{t_0})' u_1^{t_0}(y) + \sigma_1^{t_0} (u_1^{t_0})'(y).$$

Then, from the vanishing boundary condition on  $\partial B_1$  and (2.5), we arrive

$$\int_{\partial(B_2 \setminus \overline{B_1^{t_0}})} u_1^{t_0} \frac{\partial(u_1^{t_0})'}{\partial \nu^{t_0}} dS = \int_{\partial B_2} u_1^{t_0} \frac{\partial(u_1^{t_0})'}{\partial \nu^{t_0}} dS = (\sigma_1^{t_0})'. \quad (3.13)$$

Using equations (3.12), (3.13) and Green's identity

$$\int_{\partial(B_2 \setminus \overline{B_1^{t_0}})} u_1^{t_0} \frac{\partial(u_1^{t_0})'}{\partial \nu^{t_0}} dS = \int_{\partial(B_2 \setminus \overline{B_1^{t_0}})} \frac{\partial u_1^{t_0}}{\partial \nu^{t_0}} (u_1^{t_0})' dS,$$

we obtain the desired identity (1.6).  $\square$

## 4 The first Steklov–Dirichlet eigenfunction in two dimensions in bipolar coordinates

In sections 4 and 5, we deal with the first Steklov–Dirichlet eigenfunction on eccentric annuli in two dimensions. We use the bipolar coordinate system because of its convenience in solving the Laplace problem subject to boundary conditions on two circular interfaces. It is worth mentioning that the electric field concentration in composite materials has been successfully analyzed using bipolar or bispherical coordinates in [4, 23, 26, 32].

Later, in section 6, we numerically validate the monotonicity of  $\sigma_1^t$  in  $t$  for both two and three dimensions by using the series expansion of the first eigenfunction in bipolar and bispherical coordinates, respectively.

### 4.1 Bipolar coordinates

For  $x = (x_1, x_2)$  in Cartesian coordinates, we define bipolar coordinates  $(\xi, \theta) \in \mathbb{R} \times (-\pi, \pi]$  via the relation

$$(x, y) = \left( \frac{\alpha \sinh \xi}{\cosh \xi + \cos \theta}, \frac{\alpha \sin \theta}{\cosh \xi + \cos \theta} \right) \quad (4.1)$$

with the poles located at  $(\pm\alpha, 0)$ , where  $\alpha > 0$  will be defined later depending on the parameter  $t$ . We write  $x = x(\xi, \theta)$  to indicate its dependence on  $(\xi, \theta)$ , if necessary. The scale factors for the parameters  $\xi$  and  $\theta$  coincide, given by

$$h_\xi = h_\theta = \frac{\alpha}{\cosh \xi + \cos \theta}. \quad (4.2)$$

The coordinate level curves  $x(\xi, \cdot)$  and  $x(\cdot, \theta)$  define a curvilinear orthogonal frame in  $\mathbb{R}^2$ . The  $\xi$ -level curves of positive values are circles in the right half-plane, and the limiting cases  $\xi = \pm\infty$

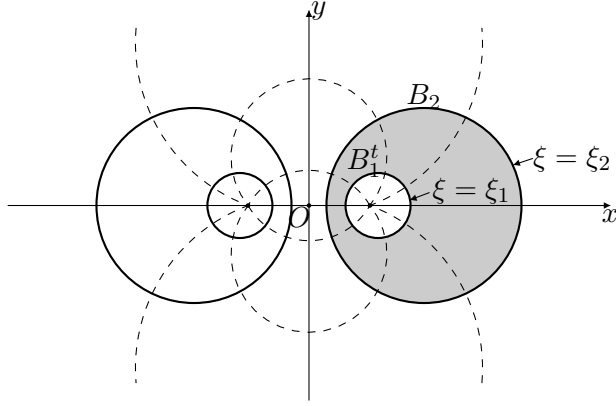


Figure 4.1:  $\xi$ -level curves (thick) and  $\theta$ -level curves (dashed) of the bipolar coordinate system. We rotate and translate the original annulus (Figure 1.1) such that  $\partial B_1^t$  and  $\partial B_2$  become  $\xi$ -level curves of some positive values ( $0 < \xi_2 < \xi_1$ ).

corresponds the poles  $(x_1, x_2) = (\pm\alpha, 0)$ . The general form of the harmonic function in bipolar coordinates, by the method of separation of variables, is

$$u(x) = a_0 + b_0\xi + \sum_{n=1}^{\infty} \left( (a_n e^{n\xi} + b_n e^{-n\xi}) \cos(n\theta) + (c_n e^{n\xi} + d_n e^{-n\xi}) \sin(n\theta) \right), \quad (4.3)$$

where  $a_n, b_n, c_n$  and  $d_n$  are constant coefficients. For a fixed  $\tilde{\xi} > 0$ , the unit normal vector at  $x(\tilde{\xi}, \theta)$  to the circle  $\xi = \tilde{\xi}$ , outward with respect to the center of the circle, is

$$\nu_{\tilde{\xi}} = \left( -\frac{1 + \cosh \tilde{\xi} \cos \theta}{\cosh \tilde{\xi} + \cos \theta}, \frac{\sinh \tilde{\xi} \sin \theta}{\cosh \tilde{\xi} + \cos \theta} \right)$$

and

$$\frac{\partial u}{\partial \nu_{\tilde{\xi}}} = -\frac{\cosh \tilde{\xi} + \cos \theta}{\alpha} \frac{\partial u}{\partial \xi} \Big|_{\xi=\tilde{\xi}}. \quad (4.4)$$

A rigid motion on a domain does not change its Steklov–Dirichlet eigenvalues. We rotate and translate the annulus  $\Omega$  (see Figure 1.1) and choose an appropriate  $\alpha > 0$  such that the inner and outer boundaries of the annulus become  $\xi$ -level curves of some positive values, namely,  $\xi_1$  and  $\xi_2$ , respectively (see Figure 4.1). Again, we call the inner disk, the outer disk and the annulus as  $B_1^t, B_2$  and  $\Omega$ , respectively. They now satisfy

$$B_1^t = t_0 e_1 + B(-te_1, r_1), \quad B_2 = t_0 e_1 + B(0, r_2) \quad \text{for some } t_0 > 0. \quad (4.5)$$

One can find that (see [4, 26] for the derivation)

$$\alpha = \frac{\sqrt{(r_2 - r_1 - t)(r_2 - r_1 + t)(r_2 + r_1 - t)(r_2 + r_1 + t)}}{2t} \quad (4.6)$$

and

$$\xi_j = \ln \left( \frac{\alpha}{r_j} + \sqrt{\left( \frac{\alpha}{r_j} \right)^2 + 1} \right), \quad j = 1, 2. \quad (4.7)$$

We note that  $0 < \xi_2 < \xi_1$  and that the interior of  $\Omega$  corresponds the rectangular region  $\xi_1 < \xi < \xi_2$ . For later use, we denote  $\varepsilon$  the distance between the inner and outer boundaries of  $\Omega$ . In other words,

$$\varepsilon := r_2 - r_1 - t.$$

If the two boundaries of  $\Omega$  are close to each other (i.e.,  $\varepsilon$  is small), we have (see [26])

$$\alpha = r_* \sqrt{\varepsilon} + O(\varepsilon \sqrt{\varepsilon}), \quad (4.8)$$

$$\xi_j = \frac{r_*}{r_j} \sqrt{\varepsilon} + O(\varepsilon \sqrt{\varepsilon}), \quad j = 1, 2, \quad (4.9)$$

with  $r_* = \sqrt{\frac{2r_1 r_2}{r_2 - r_1}}$ .

## 4.2 Series expansion of the first eigenfunction

We can analytically extend  $u_1^t$  across the boundary circles  $C_1$  and  $C_2$  on which the zero Dirichlet condition and the Robin boundary condition are assigned, respectively. We remind the reader that  $u_1^t$  does not have a sign change in  $\Omega = B_2 \setminus \overline{B_1^t}$  and  $\sigma_1$  is simple (see Lemma 2.1). The eigenfunction admits the expansion

$$u_1^t(x) = a_0 + b_0 \xi + \sum_{n=1}^{\infty} \left( a_n e^{n\xi} + b_n e^{-n\xi} \right) \cos(n\theta) \quad (4.10)$$

for some constant coefficients  $a_n$  and  $b_n$ . Indeed, since  $\Omega$  is symmetric with respect to  $x_1$ -axis,  $u_1^t(x_1, -x_2)$  is also an eigenfunction corresponding to  $\sigma_1^t$ . It therefore holds that

$$u_1^t(x_1, -x_2) = C u_1^t(x_1, x_2)$$

for some constant  $C$ . Evaluating both sides on  $x_2 = 0$  (where  $u_1^t(x_1, x_2)$  and  $u_1^t(x_1, -x_2)$  coincide and are non-zero from Lemma 2.1), we have  $C = 1$ . In other words,  $u_1^t(x_1, x_2)$  is an even function with respect to  $x_2$ -variable and, therefore, it is even with respect to  $\theta$ . Hence, in view of the general solution (4.3), we obtain (4.10). In fact, the only unknowns are  $a_n$  because of the following relation from vanishing condition on  $\partial B_1^t$  (or,  $\xi = \xi_1$ ):

$$\begin{cases} a_0 + b_0 \xi_1 = 0, \\ a_n e^{n\xi_1} + b_n e^{-n\xi_1} = 0 \quad \text{for all } n \geq 1. \end{cases} \quad (4.11)$$

**Notation 4.1.** *For notational simplicity, we define*

$$A_n(t) = n a_n e^{n\xi_1}, \quad (4.12)$$

$$\tilde{A}_n(t) = n a_n e^{n\xi_1} \cosh(n(\xi_1 - \xi_2)), \quad (4.13)$$

$$F_n(t) = \frac{\tilde{A}_{n+1}}{\tilde{A}_n}, \quad (4.14)$$

$$T_n(t) = 2 \cosh \xi_2 - \frac{2\alpha \sigma_1^t}{n} \tanh(n(\xi_1 - \xi_2)) \quad \text{for each } n \geq 1. \quad (4.15)$$

**Lemma 4.1.** Let  $\sigma_1^t$  and  $u_1^t$  be the Steklov–Dirichlet eigenfunction and the associated eigenfunction on  $\Omega = B_2 \setminus \overline{B_1^t}$ . Then, we have

$$u_1^t(x) = a_0 - \frac{a_0}{\xi_1} \xi - \sum_{n=1}^{\infty} \frac{2}{n} A_n \sinh(n(\xi_1 - \xi)) \cos(n\theta), \quad (4.16)$$

$$\left. \frac{\partial u_1^t}{\partial \xi} \right|_{\xi=\xi_2} = -\frac{a_0}{\xi_1} + \sum_{n=1}^{\infty} 2\tilde{A}_n \cos n\theta \quad (4.17)$$

and

$$\frac{d}{dt} \sigma_1^t = \frac{2\pi}{\alpha} \left( -\frac{a_0^2}{\xi_1^2} + \frac{2a_0}{\xi_1} A_1 \cosh \xi_1 - 2 \sum_{n=1}^{\infty} (A_n^2 + A_n A_{n+1} \cosh \xi_1) \right). \quad (4.18)$$

*Proof.* Using (4.10) and (4.11),  $u_1^t(x)$  is expressed as (4.16). It then follows (4.17). From (1.6), (4.2) and (4.4), we have

$$\begin{aligned} \frac{d}{dt} \sigma_1^t &= - \int_{\partial B_1^t} \left( -\frac{\partial u_1^t}{\partial \nu_{\xi_1}} \right)^2 (-\nu_{\xi_1} \cdot e_1) dS \\ &= -\frac{1}{\alpha} \int_{-\pi}^{\pi} \left( \left. \frac{\partial u_1^t}{\partial \xi} \right|_{\xi=\xi_1} \right)^2 (1 + \cosh \xi_1 \cos \theta) d\theta. \end{aligned}$$

□

**Lemma 4.2.** We can express the coefficients  $\tilde{A}_n$ , and so does  $a_n$  and  $A_n$ , in terms of  $r_1, r_2, t, \sigma_1^t$  by the recursive relation:

$$\begin{cases} \tilde{A}_1 = a_0 \frac{\cosh \xi_2}{\xi_1} - \alpha a_0 \sigma_1^t \left( 1 - \frac{\xi_2}{\xi_1} \right), \\ \tilde{A}_2 = \frac{a_0}{\xi_1} + 2\alpha \sigma_1^t \tilde{A}_1 \tanh(\xi_1 - \xi_2) - 2\tilde{A}_1 \cosh \xi_2, \\ \tilde{A}_{n+2} = -\tilde{A}_{n+1} T_{n+1} - \tilde{A}_n, \quad n \geq 1. \end{cases} \quad (4.19)$$

The constant term  $a_0$  is determined from the normalization condition (2.5). We remark that for other eigenvalues  $\sigma$ , the formulas (4.10) and (4.19) also holds with  $\sigma$  instead of  $\sigma_1^t$ .

*Proof.* On  $\partial B_2$ , it holds from the Robin boundary condition and (4.4) that

$$\sigma_1^t u_1^t \Big|_{\xi=\xi_2} = \frac{\partial u_1^t}{\partial \nu} \Big|_{\xi=\xi_2} = -\frac{\cosh \xi_2 + \cos \theta}{\alpha} \frac{\partial u_1^t}{\partial \xi} \Big|_{\xi=\xi_2}.$$

From (4.10) and (4.11), we have

$$\left. \frac{\partial u_1^t}{\partial \xi} \right|_{\xi=\xi_2} = b_0 + \sum_{n=1}^{\infty} \left( n a_n e^{n\xi_2} - n b_n e^{-n\xi_2} \right) \cos(n\theta) = -\frac{a_0}{\xi_1} + \sum_{n=1}^{\infty} 2\tilde{A}_n \cos(n\theta) \quad (4.20)$$

and, hence,

$$\begin{aligned}
& -(\cosh \xi_2 + \cos \theta) \left. \frac{\partial u_1^t}{\partial \xi} \right|_{\xi=\xi_2} \\
&= \frac{a_0 \cosh \xi_2}{\xi_1} + \frac{a_0 \cos \theta}{\xi_1} - \sum_{n=1}^{\infty} \left( 2 \tilde{A}_n \cosh \xi_2 \cos(n\theta) + \tilde{A}_n \cos(n-1)\theta + \tilde{A}_n \cos(n+1)\theta \right) \quad (4.21) \\
&= \frac{a_0 \cosh \xi_2}{\xi_1} - \tilde{A}_1 + \left( \frac{a_0}{\xi_1} - 2 \tilde{A}_1 \cosh \xi_2 - \tilde{A}_2 \right) \cos \theta - \sum_{n=2}^{\infty} \left( \tilde{A}_{n-1} + 2 \tilde{A}_n \cosh \xi_2 + \tilde{A}_{n+1} \right) \cos(n\theta). \quad (4.22)
\end{aligned}$$

On the other hand, it holds that

$$\sigma_1^t u_1^t \Big|_{\xi=\xi_2} = a_0 \sigma_1^t \left( 1 - \frac{\xi_2}{\xi_1} \right) - 2 \sigma_1^t \tilde{A}_1 \tanh(\xi_1 - \xi_2) \cos \theta - \sum_{n=2}^{\infty} \frac{2 \sigma_1^t \tilde{A}_n}{n} \tanh(n(\xi_1 - \xi_2)) \cos(n\theta).$$

We obtain the desired relations by comparing the Fourier coefficients of the two series above.  $\square$

### 4.3 Limit behavior of the ratio of consecutive coefficients $\tilde{A}_n$ (i.e., $F_n$ )

From (4.19), it holds that

$$F_n = -T_n - \frac{1}{F_{n-1}} \quad \text{for all } n \geq 2 \text{ such that } a_n \neq 0. \quad (4.23)$$

Note that  $T_n$  is not defined by  $a_n$  but is explicitly defined in terms of elementary functions. We first show some basic behaviors of  $T_n$  and  $a_n$  for sufficiently large  $n$ . We then analyze the convergence of  $F_n$ , in the aim of understanding the limit behavior of  $\tilde{A}_n$  (or,  $a_n$ ) as  $n$  goes to infinity. To state the result, we define some terminologies:

- For fixed  $t$  and  $T_n > 2$  (i.e.,  $n \geq n_0$ ), the system of two equations  $x_2 = -T_n - \frac{1}{x_1}$ ,  $x_2 = x_1$  has the two intersections  $(L_n, L_n)$  and  $(U_n, U_n)$  with (see the left graph in Figure 4.2)

$$L_n = \frac{-T_n - \sqrt{T_n^2 - 4}}{2}, \quad U_n = \frac{-T_n + \sqrt{T_n^2 - 4}}{2}. \quad (4.24)$$

- For the limiting case, the graphs of  $x_2 = -T_\infty - \frac{1}{x_1}$ ,  $x_2 = x_1$  has the two intersections  $(L_\infty, L_\infty)$  and  $(U_\infty, U_\infty)$  with

$$L_\infty = -e^{\xi_2}, \quad U_\infty = -e^{-\xi_2}.$$

One can derive these values from (4.24) with  $T_n$  replaced by  $T_\infty$ . It holds (see the right graph in Figure 4.2) that for all  $n \geq n_0$ ,

$$L_\infty < L_{n+1} < L_n < U_n < U_{n+1} < U_\infty < 0. \quad (4.25)$$

- For the case  $T_n \leq 2$  (i.e.,  $n \leq n_0 - 1$ ), we define  $L_n = U_n = -1$ .

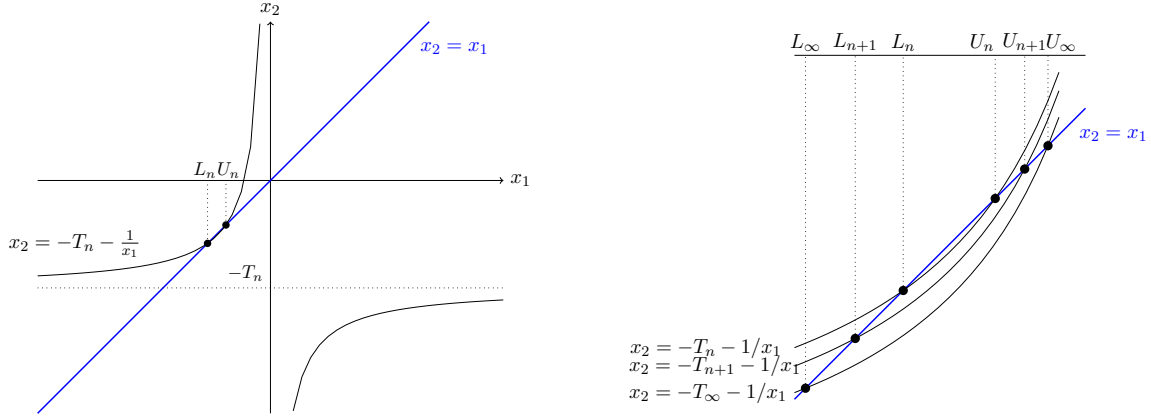


Figure 4.2: The graph of  $(x_1, x_2) = (x_1, -T_n - \frac{1}{x_1})$  (left), and illustration for  $L_{n+1} < L_n < U_n < U_{n+1}$  (right).

**Lemma 4.3.** For  $t$  arbitrary fixed in  $[0, r_2 - r_1)$ .

(a) We can choose a natural number  $n_0 = n_0(t) \geq 2$  such that

$$T_n(t) > 2 \quad \text{for all } n \geq n_0. \quad (4.26)$$

(b) If (4.26) holds, then  $a_n(t) > 0$  for all  $n \geq n_0$ .

**Lemma 4.4.** Fix  $t$  in  $[0, r_2 - r_1)$ . Let  $n_0 \in \mathbb{N}$  satisfy the properties in Lemma 4.3. We have two alternatives for the limit of  $F_n$ :

$$\lim_{n \rightarrow \infty} F_n = \begin{cases} U_\infty & \text{if } U_{n+1} < F_n < U_\infty \text{ for all } n \geq n_0, \\ L_\infty & \text{otherwise.} \end{cases} \quad (4.27)$$

We remind the reader that  $L_\infty = -e^{\xi_2}$  and  $U_\infty = -e^{-\xi_2}$ .

The proofs of Lemmas 4.3, 4.4 are provided in subsection 4.4.

#### 4.4 Proofs of Lemmas 4.3, 4.4 and Theorem 1.3

**Proof of Lemma 4.3** For all  $t$  fixed in  $[0, r_2 - r_1)$ ,  $T_n(t)$  is monotone increasing to  $T_\infty(t) := 2 \cosh \xi_2 > 2$  as  $n \rightarrow \infty$ . Hence, we can choose  $n_0$  such that (4.26) holds. Hence, we have (a).

Note that  $a_0 + b_0 \xi$  can satisfy (1.5) with  $\sigma > 0$  only when  $a_0 = b_0$ . Hence,  $a_n$  is nonzero for some  $n \geq 1$ . It implies that any two consecutive coefficients  $a_n$  and  $a_{n+1}$  cannot be both zero due to the recursive relation (4.19).

Suppose that  $a_n = 0$  (i.e.,  $\tilde{A}_n = 0$ ) for some  $n \geq n_0$ . Then, we have  $a_{n+1} \neq 0$  (i.e.,  $\tilde{A}_{n+1} \neq 0$ ). From (4.19) and (a), it holds that  $|\tilde{A}_{n+2}| > |\tilde{A}_{n+1}|$ . We also have  $|\tilde{A}_{n+3}| > 2|\tilde{A}_{n+2}| - |\tilde{A}_{n+1}| > |\tilde{A}_{n+2}|$ . Inductively, it holds that  $|\tilde{A}_{n+j+1}| > |\tilde{A}_{n+j}|$  for all  $j \geq 0$ . It contradicts the fact that the series (4.20) is convergent. Hence, we have (b).  $\square$

**Proof of Lemma 4.4** We prove the lemma by case-by-case discussions. For only Case 2-2,  $F_n$  converges to  $U_\infty$ . First, we consider the cases satisfying  $F_{n_0} < U_{n_0+1}$  (Case 1). Secondly, we consider the cases satisfying  $U_{n_0+1} < F_{n_0}$  (Case 2).

**Case 1-1** ( $F_{n_0} < L_{n_0+1}$  and  $F_n < L_{n+1}$  also for all  $n > n_0$ ). We have, for each  $n \geq n_0$ ,

$$\begin{cases} L_n = -T_n - \frac{1}{L_n} & \text{at } x_1 = L_n, \\ x_1 < -T_n - \frac{1}{x_1}, & \text{for } x_1 < L_n, \\ L_n < -T_n - \frac{1}{x_1} < x_1 & \text{for } L_n < x_1 < U_n. \end{cases} \quad (4.28)$$

From (4.23) and (4.28),  $F_n$  has a monotone increasing property:

$$F_{n+1} = -T_{n+1} - \frac{1}{F_n} > F_n \quad \text{for all } n \geq n_0. \quad (4.29)$$

On the other hand, as  $L_n$  is monotone decreasing to  $L_\infty$  and  $F_n < L_{n+1}$ ,  $F_n$  is bounded. Hence,  $F_n$  is convergent and its limit is bounded above by  $L_\infty$ .

We actually have

$$\lim_{n \rightarrow \infty} F_n = L_\infty.$$

If not, then  $F_\infty := \lim_n F_n < L_\infty$ . It implies that  $F_\infty < -T_\infty - \frac{1}{F_\infty}$ . We denote by  $\delta$  the difference between the two sides, i.e.,  $\delta = -T_\infty - \frac{1}{F_\infty} - F_\infty > 0$ . As  $F_n$  is negative and convergence, so is its reciprocal. We can take an arbitrarily large  $n$  such that  $\left| \frac{1}{F_n} - \frac{1}{F_\infty} \right| < \frac{\delta}{2}$ . We refer the reader that  $T_n$  is monotone decreasing to  $T_\infty$ . Hence, it follows that and obtain

$$F_{n+1} = -T_{n+1} - \frac{1}{F_n} > -T_\infty - \frac{1}{F_n} > -T_\infty - \frac{1}{F_\infty} - \frac{\delta}{2} = F_\infty + \frac{\delta}{2} \quad (4.30)$$

It contracts the fact that  $F_n$  converges to  $F_\infty$ .

**Case 1-2** ( $F_{n_0} < L_{n_0+1}$ , but  $F_n \geq L_{n+1}$  for some  $n > n_0$ ). Let  $n_1$  be the smallest integer satisfying that  $n_1 > n_0$  and  $F_{n_1} \geq L_{n_1+1}$ . Then, it holds that  $F_{n_1-1} < L_{n_1}$  and, by also using (4.25), that

$$F_{n_1} = -T_{n_1} - \frac{1}{F_{n_1-1}} < -T_{n_1} - \frac{1}{L_{n_1}} = L_{n_1} < U_{n_1} < U_{n_1+1}.$$

Hence,  $L_{n_1+1} \leq F_{n_1} < U_{n_1+1}$ . This case reduces to either Case 1-3 or Case 1-4.

**Case 1-3** ( $F_{n_0} = L_{n_0+1}$  or  $F_{n_0} = U_{n_0+1}$ ). We have from (4.25) and the definition of  $L_{n_0+1}$  or  $U_{n_0+1}$  that

$$L_{n_0+2} < F_{n_0+1} = F_{n_0} < U_{n_0+2}.$$

This case reduces to Case 1-4.

**Case 1-4** ( $L_{n_0+1} < F_{n_0} < U_{n_0+1}$ ). One can easily find from (4.25) and (4.28) that

$$L_{n_0+2} < L_{n_0+1} < F_{n_0+1} = -T_{n_0+1} - \frac{1}{F_{n_0}} < F_{n_0} < U_{n_0+1} < U_{n_0+2}.$$

Inductively, it holds that  $L_{n+1} < F_n < U_{n+1}$  and  $F_{n+1} < F_n$  for all  $n \geq n_0$ . Hence,  $F_n$  is convergent and its limit is bounded below by  $L_\infty$  and strictly smaller than  $U_\infty$ . We prove that the limit equals to  $L_\infty$  by a similar procedure similar to that used in Case 1-1.

If  $F_\infty := \lim_n F_n > L_\infty$ , then  $F_\infty > -T_\infty - \frac{1}{F_\infty}$ . Let

$$\delta := F_\infty + T_\infty + \frac{1}{F_\infty} > 0.$$

We can take an arbitrarily large  $n$  such that  $\left| \frac{1}{F_n} - \frac{1}{F_\infty} \right| < \frac{\delta}{4}$  and  $|T_n - T_\infty| < \frac{\delta}{4}$ . Then

$$F_{n+1} = -T_{n+1} - \frac{1}{F_n} < -T_\infty - \frac{1}{F_\infty} + \frac{\delta}{2} = F_\infty - \delta + \frac{\delta}{2} < F_\infty. \quad (4.31)$$

As  $F_n$  is monotone decreasing,  $F_n$  cannot converge to  $F_\infty$ , a contradiction.

**Cases 2-1** ( $U_{n_0+1} < F_{n_0}$  and  $F_{n_1} \leq U_{n_1+1}$  for some  $n_1 > n_0$ ). This case reduces to the previous cases by taking  $n_1$  instead of  $n_0$ .

**Cases 2-2** ( $U_{n+1} < F_n < U_\infty$  for all  $n \geq n_0$ ). Since  $U_{n+1}$  converges to  $U_\infty$ , so  $F_n$  also converges to  $U_\infty$ .

**Cases 2-3** ( $U_\infty < F_n$  for some  $n \geq n_0$  and  $F_n \leq 0$  for all  $n \geq n_0$ ). As  $U_{n+1} < U_\infty < F_n$ , it holds that

$$F_{n+1} = -T_{n+1} - \frac{1}{F_n} > F_n \quad \text{for all } n \geq n_0.$$

In other words,  $F_n$  is increasing. As it is further assumed to be negative,  $F_n$  converges, namely to  $F_\infty \leq 0$ . As  $F_n$  is a bounded sequence,  $F_n$  cannot be very close to zero in view of (4.23). Hence,  $F_\infty < 0$ . Furthermore, from the case assumption, we have  $U_\infty < F_\infty$  and, thus,  $-T_\infty - \frac{1}{F_\infty} > F_\infty$ .

Now, let

$$\delta := -T_\infty - \frac{1}{F_\infty} - F_\infty > 0.$$

For arbitrary sufficiently large  $n$ , we have  $|T_\infty - T_n| < \frac{\delta}{4}$  and  $\left| \frac{1}{F_n} - \frac{1}{F_\infty} \right| < \frac{\delta}{4}$ . Then, it follows that

$$F_{n+1} = -T_{n+1} - \frac{1}{F_n} > -T_\infty - \frac{1}{F_\infty} - \frac{\delta}{2} > F_\infty. \quad (4.32)$$

As  $F_n$  is monotone increasing,  $F_n$  cannot converge to  $F_\infty$ , a contradiction.

**Cases 2-4** ( $0 < F_n$  for some  $n \geq n_0$ ). We have  $F_{n+1} < -T_{n+1} < L_{n+1}$ . This case reduces to Case 1-1 or Case 1-2. □

**Proof of Theorem 1.3** We can analytically extend  $u_1^t$  across  $C_2$ . Hence, the right-hand side of (4.16) converges at  $\xi = \xi_2$  and, thus,

$$\begin{aligned} 1 &\geq \limsup_{n \rightarrow \infty} \left| \frac{A_{n+1} \sinh((n+1)(\xi_1 - \xi_2))}{A_n \sinh(n(\xi_1 - \xi_2))} \right| \\ &= \limsup_{n \rightarrow \infty} \frac{A_{n+1} \cosh((n+1)(\xi_1 - \xi_2))}{A_n \cosh(n(\xi_1 - \xi_2))} \\ &= \limsup_{n \rightarrow \infty} |F_n|. \end{aligned}$$

Here, we used the fact that  $\xi_1 - \xi_2$  is nonzero and independent of  $n$ . Therefore, one can eliminate  $-e^{\xi_1}$  from the two alternatives of the limit of  $F_n$ . From the case study in the proof of Lemma 4.4, the theorem follows.  $\square$

## 5 Asymptotic behavior of the first eigenvalue and eigenfunction for small distance between the two boundaries of the annulus

In this section, we assume that the distance between the two boundaries of the annulus  $\Omega$  is small, i.e.,

$$\varepsilon = r_2 - r_1 - t \ll 1.$$

Then,  $\alpha$  and  $\xi_j$  are  $O(\sqrt{\varepsilon})$  and admit the asymptotics in (4.8) and (4.9). Note that  $\sigma_1^t$  is uniformly bounded independently of  $t$  as it is positive for all  $t$  and attains a maximum at  $t_0$ .

### 5.1 Asymptotic behavior of $T_n$ and $U_n$

From Lemma 4.2, we have

$$\tilde{A}_1 = a_0 \left( \frac{1}{\xi_1} + O(\sqrt{\varepsilon}) \right), \quad \tilde{A}_2 = a_0 \left( -\frac{1}{\xi_1} + O(\sqrt{\varepsilon}) \right). \quad (5.1)$$

It then follows that

$$F_1(t) = \frac{\tilde{A}_2}{\tilde{A}_1} = -1 + O(\varepsilon). \quad (5.2)$$

We also obtain

$$\begin{aligned} T_2(t) &= 2 \cosh \xi_2 - \frac{2\alpha\sigma_1^t}{2} \tanh(2(\xi_1 - \xi_2)) \\ &= 2 \cosh \xi_2 - 2\alpha\sigma_1^t(\xi_1 - \xi_2) \frac{\tanh(2(\xi_1 - \xi_2))}{2(\xi_1 - \xi_2)} \\ &= 2 + \xi_2^2 + O(\varepsilon^2) - 2\alpha\sigma_1^t(\xi_1 - \xi_2) + O(\varepsilon^2) \\ &= 2 + \frac{2r_1}{r_2(r_2 - r_1)}\varepsilon - 4\sigma_1^t\varepsilon + O(\varepsilon^2) \end{aligned} \quad (5.3)$$

from the definition of  $T_n$ , (4.15), and the fact that  $\frac{\tanh s}{s} = 1 + O(s^2)$  and  $\frac{\tanh s}{s} \leq 1$  for  $s \geq 0$ . For general  $n$  we have the following.

**Lemma 5.1.** *For some  $\varepsilon_0 = \varepsilon_0(r_1, r_2) > 0$ , it holds for all  $\varepsilon < \varepsilon_0$  and  $n \in \mathbb{N}$  that*

$$T_n(t) = 2 + \frac{2r_1}{r_2(r_2 - r_1)} R_n(t)\varepsilon + O(\varepsilon^2), \quad (5.4)$$

$$U_n(t) = -e^{-\sqrt{R_n^+(t)}\xi_2} + O(\varepsilon) \quad (5.5)$$

with

$$R_n(t) = 1 - \sigma_1^t \frac{2r_2(r_2 - r_1)}{r_1} \frac{\tanh(n(\xi_1 - \xi_2))}{n(\xi_1 - \xi_2)}, \quad (5.6)$$

where  $O(\varepsilon)$  and  $O(\varepsilon^2)$  are uniform in  $n$  and  $a^+ := \max(a, 0)$  for  $a \in \mathbb{R}$ .

*Proof.* We have the uniform boundedness for  $R_n(t)$  thanks to  $|\frac{\tanh s}{s}| \leq 1$  and  $\sigma_1^t \leq \sigma_1^0$ ; the maximality of  $\sigma_1^t$  at  $t = 0$  was verified in [41, 20]. In other words, there exist a positive constant  $C$  independent of  $\varepsilon$  and  $n$  such that

$$|R_n(t)| \leq C \quad \text{for all } \varepsilon > 0, n \in \mathbb{N}. \quad (5.7)$$

We then estimate

$$\begin{aligned} T_n(t) &= 2 \cosh \xi_2 - 2\alpha(\xi_1 - \xi_2)\sigma_1^t \frac{\tanh(n(\xi_1 - \xi_2))}{n(\xi_1 - \xi_2)} \\ &= 2 + \xi_2^2 + O(\varepsilon^2) - 2\alpha(\xi_1 - \xi_2)\sigma_1^t \frac{\tanh(n(\xi_1 - \xi_2))}{n(\xi_1 - \xi_2)} \end{aligned} \quad (5.8)$$

$$= 2 + \frac{2r_1}{r_2(r_2 - r_1)}\varepsilon \left( 1 - \sigma_1^t \frac{2r_2(r_2 - r_1)}{r_1} \frac{\tanh(n(\xi_1 - \xi_2))}{n(\xi_1 - \xi_2)} \right) + O(\varepsilon^2). \quad (5.9)$$

Here,  $O(\varepsilon^2)$  follows from  $2 \cosh \xi_2 - 2 - \xi_2^2$ , so it is uniform in  $n$ . It proves (5.4). In the remaining, we prove (5.5).

If  $T_n(t) \leq 2$ , then  $U_n(t) = 1$  by the definition and  $R_n^+(t) = O(\varepsilon)$ . Hence, we have (5.5) for this case.

If  $T_n(t) > 2$  and  $R_n(t) < 0$ , then  $2 < T_n(t) \leq 2 + O(\varepsilon^2)$  and  $R_n^+(t) = 0$ . Hence, we have  $U_n(t) = -1 + O(\varepsilon)$  from the definition of  $U_n$  (4.24) and, thus, (5.5) holds.

If  $T_n(t) > 2$  and  $R_n(t) \geq 0$ , then (5.4) gives

$$\begin{aligned} U_n(t) &= \frac{-T_n(t) + \sqrt{T_n(t)^2 - 4}}{2} \\ &= -1 + \sqrt{\frac{2r_1}{r_2(r_2 - r_1)}} \sqrt{R_n(t)} \sqrt{\varepsilon} + O(\varepsilon) \\ &= -e^{-\sqrt{R_n(t)}\xi_2} + O(\varepsilon), \end{aligned}$$

which is the desired conclusion. □

Using Lemma 5.1, we derive a lower bound of the first eigenvalue as in the following subsection.

## 5.2 Proof of Theorem 1.4 (lower bound of $\sigma_1^t$ )

Suppose the contrary: there exist a constant  $C$  satisfying  $0 < C < 1$  and a sequence  $\{\varepsilon_j\}_{j=1}^\infty$  such that  $t_j = r_2 - r_1 - \varepsilon_j$  is in  $(0, r_2 - r_1)$ ,  $t_j \uparrow (r_2 - r_1)$ , and

$$\sigma_1^{t_j} < \frac{r_1}{2r_2(r_2 - r_1)} C \quad \text{for all } j.$$

It then holds that

$$R_3(\varepsilon_j) = 1 - \sigma_1^{t_j} \frac{2r_2(r_2 - r_1)}{r_1} \frac{\tanh(3(\xi_1^j - \xi_2^j))}{3(\xi_1^j - \xi_2^j)} \geq 1 - C > 0 \quad \text{for all } j,$$

where  $\xi_1^j$  and  $\xi_2^j$  denote the level values  $\xi_1$  and  $\xi_2$  depending on  $t_j$ . Since  $R_3(\varepsilon) > 0$ , we have from (5.5) that

$$\begin{aligned} U_3(t_j) &= -1 + \sqrt{R_3(\varepsilon_j)} \sqrt{\frac{2r_1}{r_2(r_2 - r_1)}} \sqrt{\varepsilon_j} + O(\varepsilon_j) \\ &\geq -1 + \sqrt{1 - C} \sqrt{\frac{2r_1}{r_2(r_2 - r_1)}} \sqrt{\varepsilon_j} + O(\varepsilon_j). \end{aligned} \quad (5.10)$$

From (5.3), we have

$$T_2(t_j) > 2 \quad \text{for all } j.$$

It then follows from Theorem 1.3, (5.3) and (5.2) that

$$U_3(t_j) < F_2(t_j) = -T_2(t_j) - \frac{1}{F_1(t_j)} = -1 + O(\varepsilon_j). \quad (5.11)$$

It contradicts the inequality (5.10).  $\square$

**Remark 1.** For the domain  $B(0, 1) \setminus \bar{A}$  which is conformally equivalent to the Grötzsch ring  $R_G(r) := B(0, 1) \setminus ([0, r] \times \{0\})$  for some  $0 < r < 1$ , Dittmar and Solynin showed in [16] that

$$\sigma_1(B(0, 1) \setminus \bar{A}) \geq \sigma_1(R_G(r)). \quad (5.12)$$

It is well-known that  $\sigma_1(R_G(r)) < \frac{1}{2}$  for all  $r$ . Therefore, we have

$$\frac{r_1}{2r_2(r_2 - r_1)} > \frac{1}{2} > \sigma_1(R_G(r)) \quad \text{for } r_2 = 1, r_1 > 1/2.$$

We highlight that the bound in (1.7) is larger than that in (5.12) when  $\frac{r_1}{r_2} > \frac{1}{2}$  and the two boundaries of an annulus are sufficiently close.

### 5.3 Asymptotic behavior of $F_n$

In this subsection, we further estimate the coefficient ratio  $F_n$ , given that  $\varepsilon \ll 1$  and that  $r_1/r_2$  is contained in a certain interval; see Theorem 5.2. While Theorem 1.3 holds only for  $n \geq n_0$  with some  $n_0 = n_0(t) \in \mathbb{N}$ , (5.18) holds for all  $n \geq 1$ .

**Notation 5.1.** For  $\varepsilon > 0$ , we define

$$\begin{aligned} N(\varepsilon) &:= \sup \{n : R_n(t) \leq 0\}, \\ C_0(\varepsilon) &:= \sup_{s \leq \varepsilon} \sqrt{s} N(s), \end{aligned} \quad (5.13)$$

$$C_1(\varepsilon) := -\frac{2r_1}{r_2(r_2 - r_1)} R_1(\varepsilon). \quad (5.14)$$

Remind that

$$R_n(t) = 1 - \sigma_1^t \frac{2r_2(r_2 - r_1)}{r_1} \frac{\tanh(n(\xi_1 - \xi_2))}{n(\xi_1 - \xi_2)}$$

and

$$\sigma_1^t \frac{2r_2(r_2 - r_1)}{r_1} = \text{ord}(1),$$

where  $f = \text{ord}(1)$  means that there exist constants  $c_1, c_2 > 0$  independent of  $\varepsilon$  (i.e., independent of  $t$ ) such that  $c_1 \leq f \leq c_2$ . By the same way we define  $\text{ord}(\varepsilon)$  and  $\text{ord}(\sqrt{\varepsilon})$ . As  $\frac{\sinh s}{s}$  attains 1 at  $s = 0$  and decreases to zero as  $s \rightarrow \infty$ , there is a positive constant  $s_0$  independent of  $\varepsilon$  such that  $R_n(t) > 0$  if  $n(\xi_1 - \xi_2) > s_0$ . As  $\xi_1$  and  $\xi_2$  are  $\text{ord}(\sqrt{\varepsilon})$ , we have

$$N(\varepsilon) = O\left(\frac{1}{\sqrt{\varepsilon}}\right) \quad \text{and} \quad C_0 = \text{ord}(1). \quad (5.15)$$

**Theorem 5.2.** *Let  $\Omega$  be an eccentric annulus in two dimensions satisfying (see subsection 5.4 for the validation of this condition) that for sufficiently small  $\tilde{\varepsilon}$ ,*

$$C_0^2(\tilde{\varepsilon})C_1(\varepsilon) < 1.329 \quad \text{for all } \varepsilon \leq \tilde{\varepsilon}. \quad (5.16)$$

*Then, for  $t$  such that  $\varepsilon = r_2 - r_1 - t$  is sufficiently small, we have*

$$a_n \neq 0 \quad \text{and} \quad F_n < 0 \quad \text{for all } n \geq 1. \quad (5.17)$$

*Furthermore, for any  $\delta > 0$ , there exists  $\varepsilon_0 > 0$  such that*

$$-e^{-\sqrt{R_n^+(\varepsilon)}\xi_2} - \delta\sqrt{\varepsilon} \leq F_n(\varepsilon) \leq -e^{-\xi_2} \quad \text{for all } n \geq 1, \varepsilon \leq \varepsilon_0. \quad (5.18)$$

*Proof.* From (5.5) and Theorem 1.3, we have the desired property for  $n$  satisfying  $T_n(t) > 2$ . In the remaining we prove (5.17) and (5.18) for the case  $T_n(t) < 2$ , i.e.,  $n \leq N(\varepsilon)$ .

We first prove (5.17) by using the fact that

$$F_n < 0 \quad \text{if } a_k \neq 0 \text{ for all } k \leq n. \quad (5.19)$$

We know  $a_0, a_1, a_2 \neq 0$ . Suppose that  $a_n = 0$  for some  $3 \leq n \leq N(\varepsilon)$  and  $a_k \neq 0$  for all  $k < n$ . Then, we must have  $F_{n-1} = 0$  from its definition, which contradicts (5.19). Hence,  $a_n$  is nonzero, and it proves (5.17).

Now, we prove (5.19). Note that  $T_1 = 2 - C_1\varepsilon + O(\varepsilon^2)$ . We define a function

$$f(x) := -\frac{1}{x} - T_1 = -\frac{1}{x} - (2 - C_1\varepsilon) + O(\varepsilon^2) \quad \text{for } x < 0$$

and define  $x_n$  such that  $f^{(n-1)}(x_n) = -\frac{1}{2}$ , where  $f^{(n-1)}$  denotes the  $(n-1)$ -multiple composition of  $f$  and  $f^{(0)}$  is the identity function. We claim that

$$x_n \geq -\frac{n}{n+1} - \frac{99}{100C_0^2}n\varepsilon \quad \text{for all } 1 \leq n \leq N(\varepsilon). \quad (5.20)$$

For  $n = 1$ , we have  $x_1 = -\frac{1}{2}$ , which satisfies (5.20). We set  $B(t)$  such that  $T_1 = 2 - C_1\varepsilon + B(t)\varepsilon^2$ . Note that  $B(t) = O(1)$ . Assuming (5.20) for  $n = k$ , we obtain

$$\begin{aligned} -x_k - T_1 &\leq \frac{k}{k+1} + \frac{99}{100C_0^2}k\varepsilon - 2 + C_1\varepsilon - B(t)\varepsilon^2 \\ &= -\frac{k+2}{k+1} + \frac{99}{100C_0^2}k\varepsilon + C_1\varepsilon - B(t)\varepsilon^2. \end{aligned} \quad (5.21)$$

We have

$$\begin{aligned}
& \left( -\frac{k+2}{k+1} + \frac{99}{100C_0^2}k\varepsilon + C_1\varepsilon - B(t)\varepsilon^2 \right) \left( -\frac{k+1}{k+2} - \frac{99}{100C_0^2}(k+1)\varepsilon \right) \\
&= 1 + \frac{99}{100C_0^2}(k+2)\varepsilon - \frac{99}{100C_0^2} \frac{k(k+1)}{k+2} \varepsilon - \left( \frac{99}{100C_0^2} \right)^2 k(k+1)\varepsilon^2 \\
&\quad - \frac{k+1}{k+2}C_1\varepsilon - \frac{99}{100C_0^2}C_1(k+1)\varepsilon^2 + \frac{k+1}{k+2}B(t)\varepsilon^2 + \frac{99B(t)}{100C_0^2}(k+1)\varepsilon^3 \\
&\geq 1 + \varepsilon \left( \frac{99}{100C_0^2} \cdot \frac{3k+4}{k+2} - \left( \frac{99}{100C_0^2} \right)^2 \times C_0^2 - C_1 \right) + O(\varepsilon\sqrt{\varepsilon}) \\
&> 1 + \varepsilon \left( \frac{99}{100C_0^2} \cdot \frac{7}{3} - \left( \frac{99}{100} \right)^2 \cdot \frac{1}{C_0^2} - 1.329 \cdot \frac{1}{C_0^2} \right) + O(\varepsilon\sqrt{\varepsilon}) > 1. \tag{5.22}
\end{aligned}$$

We use  $k \leq N(\varepsilon) \leq \frac{C_0}{\sqrt{\varepsilon}}$  in the first inequality and (5.16) in the second inequality. From (5.21), (5.22) and the fact that  $f(x_{k+1}) = x_k$ , it follows

$$\frac{1}{x_{k+1}} = -x_k - T_1 \leq \frac{1}{-\frac{k+1}{k+2} - \frac{99}{100C_0^2}(k+1)\varepsilon}.$$

Hence, it follows (5.20) for  $n = k + 1$ . From (5.20),

$$\begin{aligned}
x_{N(\varepsilon)} &\geq -\frac{N(\varepsilon)}{N(\varepsilon)+1} - \frac{99}{100C_0^2}N(\varepsilon)\varepsilon \\
&= -1 + \frac{1}{N(\varepsilon)+1} - \frac{99}{100C_0^2}N(\varepsilon)\varepsilon \geq -1 + \left( \frac{1}{100C_0} \right) \sqrt{\varepsilon} + O(\varepsilon),
\end{aligned}$$

and it is bigger than  $F_1 = -1 + O(\varepsilon)$ . Hence, we have

$$F_1 \leq x_{N(\varepsilon)}. \tag{5.23}$$

Note that

$$F_n = -T_n - \frac{1}{F_{n-1}} \leq -T_1 - \frac{1}{F_{n-1}} = f(F_{n-1}). \tag{5.24}$$

It then directly follows from (5.24) and (5.23) that

$$F_n \leq f(F_{n-1}) \leq f^2(F_{n-2}) \leq \dots \leq f^{(n-1)}(F_1) \leq -\frac{1}{2} < 0.$$

Hence, we prove (5.19).

Equation (4.23) implies that

$$F_n(\varepsilon) \leq F_{n+1}(\varepsilon) \quad \text{for all } 1 \leq n \leq N(\varepsilon). \tag{5.25}$$

We remind the reader that  $F_1(t) = -1 + O(\varepsilon)$  and that  $F_{N(\varepsilon)+1}$  is bounded by  $-e^{-\xi_2}$ . From the monotonicity (5.25), it holds that

$$-1 + O(\varepsilon) = F_1(\varepsilon) \leq F_2(\varepsilon) \leq \dots \leq F_{N(\varepsilon)}(\varepsilon) \leq F_{N(\varepsilon)+1}(\varepsilon) \leq -e^{-\xi_2}. \tag{5.26}$$

Moreover, we have from (5.9) that

$$R_n(\varepsilon) \leq C\varepsilon \quad \text{for all } 1 \leq n \leq N(\varepsilon)$$

for some constant  $C$ . It implies that

$$-e^{-\sqrt{R_n^+(\varepsilon)}\xi_2} = -1 + O(\varepsilon) \quad \text{for all } 1 \leq n \leq N(\varepsilon), \quad (5.27)$$

where  $O(\varepsilon)$  is independent of  $n$ . The relations (5.26) and (5.27) imply (5.18). Hence, we finish the proof of the theorem.  $\square$

#### 5.4 Validation of the condition (5.16) in Theorem 5.2

In this subsection, we perform numerical calculations to replace the condition (5.16) by a magnitude condition on the radius ratio  $\frac{r_1}{r_2}$ .

We set

$$g(s) := \frac{\tanh s}{s} \quad \text{for } s > 0,$$

which is strictly decreasing in  $s$ , and find that  $n \leq N(\varepsilon)$  iff  $\frac{r_1}{2r_2(r_2-r_1)\sigma_1^t} \leq g(n(\xi_1 - \xi_2))$ . Then, it holds that

$$\begin{aligned} C_0(\tilde{\varepsilon}) &= \sup_{\varepsilon \leq \tilde{\varepsilon}} \sqrt{\varepsilon} N(\varepsilon) \leq \sup_{\varepsilon \leq \tilde{\varepsilon}} \frac{\sqrt{\varepsilon}}{\xi_1 - \xi_2} g^{-1}\left(\frac{r_1}{2r_2(r_2 - r_1)\sigma_1^t}\right) \\ &\leq \sqrt{\frac{r_1 r_2}{2(r_2 - r_1)}} g^{-1}\left(\frac{r_1}{2r_2(r_2 - r_1)\sigma_1^t}\right) + O(\tilde{\varepsilon}). \end{aligned}$$

By using the fact that  $C_1(\varepsilon) < -\frac{2r_1}{r_2(r_2-r_1)} + 4\sigma_1^t$ , we obtain

$$C_0^2(\tilde{\varepsilon})C_1(\varepsilon) \leq h\left(\frac{r_1}{r_2}, \sigma_1^t\right) + O(\tilde{\varepsilon}) \quad (5.28)$$

with

$$h\left(\frac{r_1}{r_2}, \lambda\right) := \frac{r_1 r_2}{2(r_2 - r_1)} \left( g^{-1}\left(\frac{r_1}{2r_2(r_2 - r_1)\lambda}\right) \right)^2 \left( 4\lambda - \frac{2r_1}{r_2(r_2 - r_1)} \right). \quad (5.29)$$

The right-hand side in (5.29) is defined in terms of elementary functions depending on  $\frac{r_1}{r_2}$  and  $\lambda$ , and one can easily find from (5.28) and (5.29) that the condition (5.16) holds for sufficiently small  $\tilde{\varepsilon}$  if we show  $h(\frac{r_1}{r_2}, \sigma_1^t) < 1.328$  for  $t$  satisfying  $\varepsilon = r_2 - r_1 - t \ll 1$ .

Since  $h$  is monotone increasing with respect to  $\lambda > \frac{r_1}{2r_2(r_2-r_1)}$ , we can derive an upper bound of  $h(\frac{r_1}{r_2}, \sigma_1^t)$  by using an upper bound of  $\sigma_1^t$ . In particular, we use  $M(t)$  given by (2.11). Moreover, since  $h(\frac{r_1}{r_2}, M(t))$  is continuous in  $t$ , we just need to numerically evaluate at  $\lambda = M(r_2 - r_1)$  to see the behavior of  $h$  for  $\varepsilon \ll 1$ . Figure 5.1 clearly shows by numerical evaluation that

$$h\left(\frac{r_1}{r_2}, M(r_2 - r_1)\right) < 1.328 \quad \text{for } 0.216 < \frac{r_1}{r_2} < 0.315.$$

Hence, we arrive the following.

**Computational conclusion:** Assume  $0.216 < \frac{r_1}{r_2} < 0.315$ , then the condition (5.16) holds for sufficiently small  $\tilde{\varepsilon}$ .

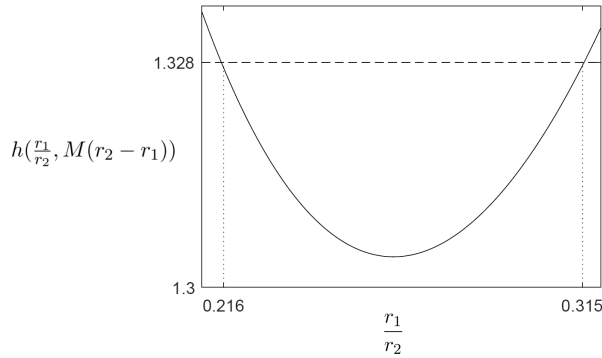


Figure 5.1: Graph of  $h(\frac{r_1}{r_2}, M(r_2 - r_1))$ , i.e.,  $\varepsilon = 0$ , where  $M(t)$  is the upper bound of  $\sigma_1^t$  given by (2.11).

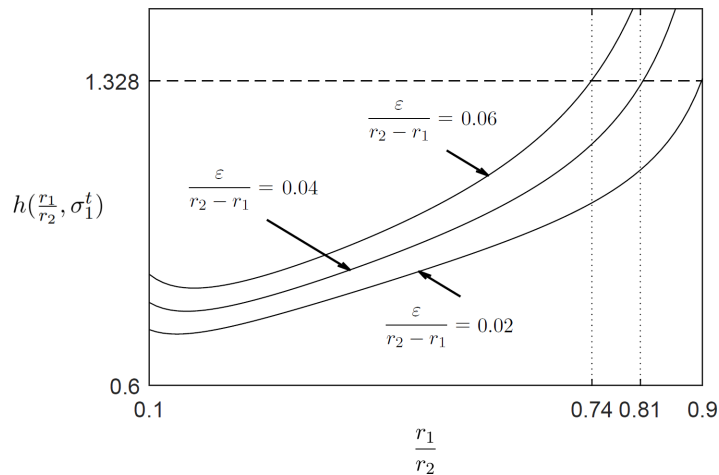


Figure 5.2: Graph of  $h(\frac{r_1}{r_2}, \sigma_1^t)$  against  $\frac{r_1}{r_2}$  with  $\frac{\varepsilon}{r_2 - r_1} = 0.06, 0.04, 0.02$ , where  $\sigma_1^t$  is numerically computed by the method described in subsection 6.1. This suggests a more relaxed condition on  $\frac{r_1}{r_2}$  than those obtained by using  $M(t)$ .

**Remark 2.** Figure 5.2 shows the numerical computation of  $h(\frac{r_1}{r_2}, \sigma_1^t)$  for  $0.1 \leq \frac{r_1}{r_2} \leq 0.9$  and  $\frac{\varepsilon}{r_2 - r_1} = 0.06, 0.04, 0.02$ , where  $\sigma_1^t$  is obtained by the numerical method described in subsection 6.1. We exclude the small or large  $\frac{r_1}{r_2}$  to have a sufficient accuracy in the numerical computation. This suggests a more relaxed condition on  $\frac{r_1}{r_2}$  than those obtained by using the upper bound  $M(t)$  given in (2.11).

## 6 Numerical computation

We numerically compute the first Steklov–Dirichlet eigenvalue on annuli with various  $r_1, r_2$  and  $t$  in two and three dimensions. Numerical results support the conjecture that  $\sigma_1^t$  is monotone decreasing as a function of  $t$ .

## 6.1 Two dimensions

We compute  $\sigma_1^t$  by using the bipolar coordinates. Recall that  $\sigma_1^t$  is the first eigenvalue of the Dirichlet-to-Neumann operator  $L$  on  $C^\infty(C_2)$  (see (2.2)). By Lemma 4.1, the corresponding eigenfunction  $u_1^t$  is an even function with respect to the bipolar coordinate  $\theta$ . We denote by  $C_e^\infty(C_2)$  the collection of even functions in  $C^\infty(C_2)$ . We also derive  $L(C_e^\infty(C_2)) \subset C_e^\infty(C_2)$  from (4.4) and the cosine part of (4.3). Because of  $u_1^t \in C_e^\infty(C_2)$ , the first eigenvalue of the restriction  $L|_{C_e^\infty(C_2)}$  is the same as  $\sigma_1^t$ .

We note that each function in  $C_e^\infty(C_2)$  admits a cosine series expansion. It directly follows from (4.11) and (4.22) that

$$L \left[ a_0 - \frac{a_0}{\xi_1} \xi_2 - \sum_{n=1}^{\infty} 2a_n e^{\xi_1} \sinh(n(\xi_1 - \xi_2)) \cos(n\theta) \right] = \frac{1}{\alpha} \left( \frac{a_0 \cosh \xi_2}{\xi_1} - \tilde{A}_1 \right. \\ \left. + \left( \frac{a_0}{\xi_1} - 2\tilde{A}_1 \cosh \xi_2 - \tilde{A}_2 \right) \cos \theta - \sum_{n=2}^{\infty} \left( \tilde{A}_{n-1} + 2\tilde{A}_n \cosh \xi_2 + \tilde{A}_{n+1} \right) \cos(n\theta) \right)$$

with

$$\tilde{A}_n = na_n e^{n\xi_1} \cosh(n(\xi_1 - \xi_2)).$$

One can replace the coefficients  $a_n$  by any numbers as long as the series converges. In particular, we have

$$L[1] = \frac{1}{\alpha(\xi_1 - \xi_2)} [\cosh \xi_2 + \cos \theta], \\ L[\cos \theta] = \frac{1}{2\alpha \tanh(\xi_1 - \xi_2)} [1 + 2 \cosh \xi_2 \cos \theta + \cos(2\theta)], \\ L[\cos(k\theta)] = \frac{k}{2\alpha \tanh(k(\xi_1 - \xi_2))} [\cos((k-1)\theta) + 2 \cosh \xi_2 \cos(k\theta) + \cos((k+1)\theta)], \quad k \geq 2.$$

We define an inner-product  $(\cdot, \cdot)$  on  $C_e^\infty(C_2)$  by

$$(\cos(m\theta), \cos(k\theta)) = d_k^2 \delta_{mn} \tag{6.1}$$

with

$$d_k^2 = \begin{cases} \frac{1}{\xi_1 - \xi_2} & \text{if } k = 0, \\ \frac{k}{2 \tanh(k(\xi_1 - \xi_2))} & \text{otherwise,} \end{cases} \tag{6.2}$$

where the symbol  $\delta_{mk}$  denotes the Kronecker's delta. Then, the operator  $L$  is symmetric

The main idea of the numerical calculation of  $\sigma_1^t$  is to consider  $P_n L P_n$  instead of  $L$ , where  $P_n$  is a natural projection operator from  $C_e^\infty(C_2)$  onto the  $n$ -dimensional subspace

$$H_n := \text{span} \{ \cos(k\theta) : k = 1, \dots, n-1 \}.$$

The finite section operators  $P_nLP_n$ , for example,

$$P_3LP_3 \left[ \sum_{k=0}^{\infty} c_k \cos(k\theta) \right] \\ = \begin{pmatrix} 1 \\ \cos(\theta) \\ \cos(2\theta) \end{pmatrix}^T \frac{1}{\alpha} \begin{pmatrix} \cosh \xi_2 \cdot d_0^2 & d_1^2 & 0 \\ d_0^2 & 2 \cosh \xi_2 \cdot d_1^2 & d_2^2 \\ 0 & d_1^2 & 2 \cosh \xi_2 \cdot d_2^2 \end{pmatrix} \begin{pmatrix} c_0 \\ c_1 \\ c_2 \end{pmatrix},$$

are symmetric with respect to the inner-product (6.1) and tridiagonal. In terms of the orthogonal basis  $\left\{ \frac{\cos(k\theta)}{d_k} \right\}$  of  $H_n$  with respect to  $(\cdot, \cdot)$ , the operator  $P_3LP_3$  is now identical to

$$\frac{1}{\alpha} \begin{pmatrix} d_0 & 0 & 0 \\ 0 & d_1 & 0 \\ 0 & 0 & d_2 \end{pmatrix} \begin{pmatrix} \cosh \xi_2 \cdot d_0^2 & d_1^2 & 0 \\ d_0^2 & 2 \cosh \xi_2 \cdot d_1^2 & d_2^2 \\ 0 & d_1^2 & 2 \cosh \xi_2 \cdot d_2^2 \end{pmatrix} \begin{pmatrix} \frac{1}{d_0} & 0 & 0 \\ 0 & \frac{1}{d_1} & 0 \\ 0 & 0 & \frac{1}{d_2} \end{pmatrix} \\ = \frac{1}{\alpha} \begin{pmatrix} \cosh \xi_2 \cdot d_0^2 & d_0 d_1 & 0 \\ d_0 d_1 & 2 \cosh \xi_2 \cdot d_1^2 & d_1 d_2 \\ 0 & d_1 d_2 & 2 \cosh \xi_2 \cdot d_2^2 \end{pmatrix}. \quad (6.3)$$

We denote by  $\sigma_{1,n}^t$  the first eigenvalue of  $P_nLP_n$ . We also set  $u_{1,n}^t$  to be a function in bipolar coordinates of series form (4.18) satisfying (4.11) whose coefficient are given by the first eigenvector of  $P_nLP_n$ . As  $P_nLP_n$  is identical to a finite dimensional matrix, one can easily compute  $\sigma_{1,n}^t$  and  $u_{1,n}^t$ .

**Lemma 6.1.** *For fixed  $t$ ,  $\{\sigma_{1,n}^t\}_{n=1}^{\infty}$  is a decreasing sequence of positive numbers.*

From this lemma,  $\sigma_{1,n}^t$  converges. We then can derive lower and upper bounds of  $\sigma_1^t$  by applying the variational formulation of the first eigenvalue for  $L$  and  $P_nLP_n$ . We refer the reader to see Appendix A for the proofs of Lemma 6.1 and Proposition 6.2.

**Proposition 6.2.** *For any  $m \in \mathbb{N}$ , it holds that*

$$\lim_{n \rightarrow \infty} \sigma_{1,n}^t \leq \sigma_1^t \leq \frac{\int_{\Omega} |\nabla u_{1,m}^t|^2 dx}{\int_{\partial\Omega} |u_{1,m}^t|^2 dS}. \quad (6.4)$$

In the following examples, we visualize the first Steklov–Dirichlet eigenvalue on various annuli, where the eigenvalue  $\sigma_1^t$  is numerically computed by the following two-step procedure:

- **Step 1.** We numerically compute  $\lim_{n \rightarrow \infty} \sigma_{1,n}^t$  by evaluating  $\sigma_{1,n}^t$  with a sufficiently large truncation size  $n$ . More precisely, we iteratively compute  $\sigma_{1,n}^t$ , where  $n$  is doubled from the initial value  $2^3$  (i.e.,  $n = 2^k$  for some  $k \geq 3$ ) until the stopping criterion

$$\left| \sigma_{1,2^{k-1}}^t - \sigma_{1,2^k}^t \right| < 10^{-12} \quad (6.5)$$

is met. For all the examples in this subsection, this stopping condition is satisfied at  $k \leq 8$ . Table 1 shows the relative error for some example annuli.

- **Step 2.** Let  $N = 2^k$  be the truncation size obtained in Step 1, which satisfies (6.5). In this second step, we validate that  $\sigma_{1,N}^t$  also approximates  $\sigma_1^t$  as well as  $\lim_{n \rightarrow \infty} \sigma_{1,n}^t$ . We gradually increase the truncation size  $n$  and evaluate the upper bound of  $\sigma_1^t$  in (6.4). For all the examples in this subsection, the difference between the upper bound and  $\sigma_{1,N}^t$  decreases and eventually satisfies

$$E_{m,N} := \left| \sigma_{1,N}^t - \frac{\int_{\Omega} |\nabla u_{1,m}^t|^2 dx}{\int_{\partial\Omega} |u_{1,m}^t|^2 dS} \right| < 10^{-12}. \quad (6.6)$$

Consequently, in view of (6.4),  $\sigma_{1,N}^t$  approximates  $\sigma_1^t$ . Figure 6.1 shows the graph of  $E_{m,N}$  against  $n$  for an annulus example.

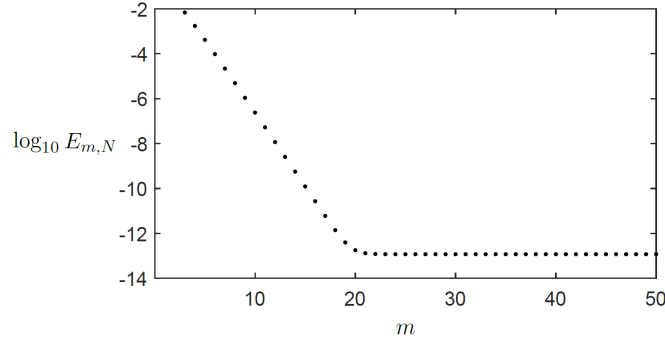


Figure 6.1: The log-scale graph of  $E_{m,N}$  against  $m$  for  $r_1 = 1$ ,  $r_2 = 3$ ,  $t = 1.2$  and  $N = 2^6$ , where  $E_{m,N}$  decreases exponentially until it reaches the relative error threshold (6.5).

In the following two examples, the eigenvalue is numerically computed by the two-step procedure explained before. We use the analytic result for the concentric case (i.e.,  $t = 0$ ). We note that the first Steklov–Dirichlet eigenvalue is invariant under the rescaling the size of the domain. In the second example, we visualize  $\sigma_1^t$  for various annuli, where  $r_2$  is fixed to be 1. The numerical results support the conjecture that  $\sigma_1^t$  is monotone decreasing as  $t$  increases.

**Example 1.** Figure 6.2 plots  $\sigma_1^t$  of the annulus in two dimensions with  $r_1 = 1$ ,  $r_2 = 3$  and  $\frac{t}{r_2 - r_1} = 0, 0.02, 0.04, \dots, 0.98$  (50 cases), where the asymptotic lower bound obtained in Theorem 1.4 is  $\frac{1}{12}$ . Table 1 shows the relative error  $\left| \sigma_{1,2^{k-1}}^t - \sigma_{1,2^k}^t \right|$  for some annuli in this figure.

**Example 2.** Figure 6.3 plots the eigenvalues for the annuli in two dimensions given by  $r_2 = 1$ ,  $r_1 = 0.2, 0.4, 0.6, 0.8$  and  $\frac{t}{r_2 - r_1} = 0, 0.02, 0.04, \dots, 0.98$ .

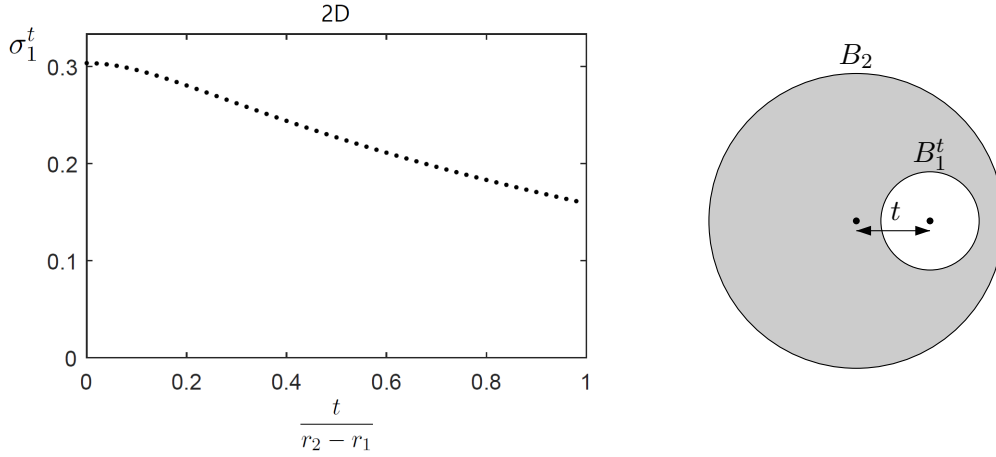


Figure 6.2: The first Steklov–Dirichlet eigenvalue for the two dimensional annulus  $B_2 \setminus \overline{B_1^t} \subset \mathbb{R}^2$  with  $r_1 = 1$ ,  $r_2 = 3$  and  $\frac{t}{r_2 - r_1} = 0, 0.02, \dots, 0.98$  (50 cases). All the cases except  $t = 0$  is numerically computed following the stopping criterion (6.5); at  $t = 0$ , we plot the exact reference eigenvalue  $(r_2(\ln r_2 - \ln r_1))^{-1}$ . The numerical values of all cases comply with the conjecture that  $\sigma_1^t$  is monotone decreasing in  $t$ .

$\frac{t}{r_2 - r_1}$	$k$	$\sigma_{1,2^k}^t$	$\sigma_{1,2^{k-1}}^t - \sigma_{1,2^k}^t$
0.2	3	0.280415816567	
	4	0.280415816560	7.32098E-12
	5	0.280415816559	2.67508E-13
0.4	3	0.243981453018	
	4	0.243981314075	1.38943E-07
	5	0.243981314075	1.20820E-13
0.6	3	0.211232489807	
	4	0.211194760285	3.77295E-05
	5	0.211194759856	4.29199E-10
	6	0.211194759856	4.91829E-14

$\frac{t}{r_2 - r_1}$	$k$	$\sigma_{1,2^k}^t$	$\sigma_{1,2^{k-1}}^t - \sigma_{1,2^k}^t$
0.8	3	0.185487114250	
	4	0.183172148523	2.31497E-03
	5	0.183167795557	4.35297E-06
	6	0.183167795551	6.58637E-12
	7	0.183167795551	4.10783E-15
0.98	3	0.359778077514	
	4	0.191032748174	1.68745E-01
	5	0.162471199179	2.85615E-02
	6	0.161289731970	1.18147E-03
	7	0.161288441910	1.29006E-06
	8	0.161288441909	7.36411E-13

Table 1: Relative errors for some annuli considered in Figure 6.2. As  $\partial B_1^t$  gets closer to  $\partial B_2$  (i.e.,  $t$  increases), we need a bigger truncated matrix to satisfy the stopping criterion (6.5).

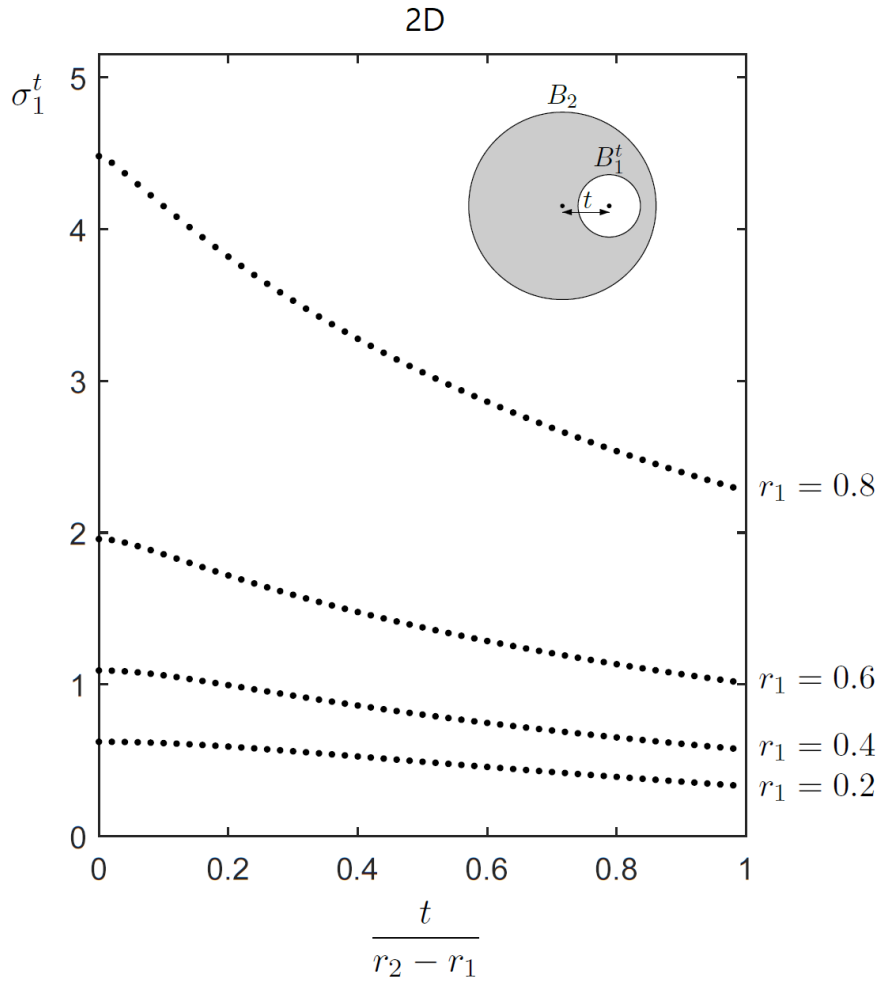


Figure 6.3: Numerical values of  $\sigma_1^t$  for various possible values of  $r_1$  and  $t$  in two dimensions, where  $r_2$  is fixed to be 1. The numerical values of all cases comply with the conjecture that  $\sigma_1^t$  is monotone decreasing in  $t$ .

## 6.2 Three dimensions

We compute  $\sigma_1^t$  by using the bippherical coordinates. Similar to the two dimensions, we use the finite section method; see Appendix B for the definition of the finite dimensional subspace and the corresponding projection operator, namely  $Q_n$ . We denote  $\sigma_{1,n}^t$  be the first eigenvalue of  $Q_n L Q_n$ , which is a tridiagonal matrix. We expect that a similar result to Lemma 6.2 holds for the three dimensions.

In the following, we compute  $\sigma_{1,n}^t$  with a sufficiently large number  $n$  such that the stopping condition (6.5) satisfied.

**Example 3.** *Figure 7.1 plots  $\sigma_1^t$  of the annulus in three dimensions with  $r_1 = 1, r_2 = 3$  and  $\frac{t}{r_2-r_1} = 0, 0.02, \dots, 0.98$  (50 cases). Table 2 shows the relative error  $\left| \sigma_{1,2^{k-1}}^t - \sigma_{1,2^k}^t \right|$  for some annuli in this figure.*

**Example 4.** *Figure 7.2 plots the eigenvalues for the annuli in three dimensions given by  $r_2 = 1, r_1 = 0.2, 0.4, 0.6, 0.8$  and  $\frac{t}{r_2-r_1} = 0, 0.02, 0.04, \dots, 0.98$ .*

## 7 Conclusion

We investigated the first Steklov–Dirichlet eigenvalue of a domain bounded by two balls of given radii and its monotonicity with respect to the distance between the two centers. We proved the differentiability of the eigenvalue and obtained an integral expression for the derivative value. For the planar annulus case, we estimated the ratio of consecutive coefficients,  $F_n$ , in the series expansion of the first eigenvalue in bipolar coordinates. As an application of this estimate, we derived an explicit lower bound of the first eigenvalue given that two circular boundaries of annulus are sufficiently close. We performed numerical computations in two and three dimensions to numerically verify the monotonicity of the first eigenvalue. The estimate on  $F_n$  may lead to analytical proof for the shape monotonicity of first Steklov–Dirichlet eigenvalue on eccentric annulus. The monotonicity is about comparing the two first eigenvalues for eccentric annuli, so it might be necessary to measure the asymmetry of the domains to prove the property.

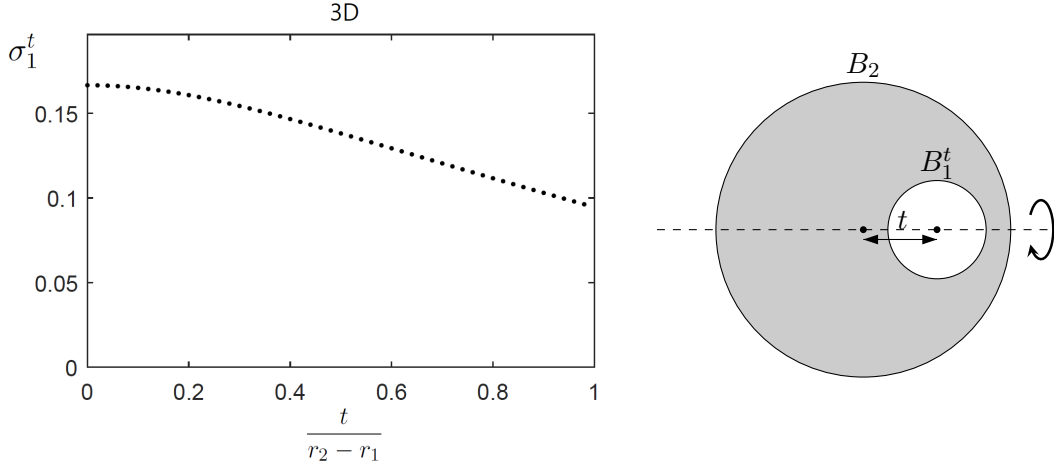


Figure 7.1: The first Steklov–Dirichlet eigenvalue for the two dimensional annulus  $B_2 \setminus \overline{B_1^t} \subset \mathbb{R}^3$  with  $r_1 = 1$ ,  $r_2 = 3$  and  $\frac{t}{r_2 - r_1} = 0, 0.02, \dots, 0.98$  (50 cases). All the cases except  $t = 0$  is numerically computed following the stopping criterion (6.5); at  $t = 0$ , we plot the exact reference eigenvalue  $\sigma_1^0 = \frac{r_1}{r_2(r_2 - r_1)}$ . The numerical values of all cases comply with the conjecture that  $\sigma_1^t$  is monotone decreasing in  $t$ .

$\frac{t}{r_2 - r_1}$	$k$	$\sigma_{1,2^k}^t$	$\sigma_{1,2^{k-1}}^t - \sigma_{1,2^k}^t$	
0.2	3	0.160816203740		
	4	0.160816203735	5.35158E-12	
	5	0.160816203735	6.38656E-14	
0.4	3	0.146672847283		
	4	0.146672620433	2.26850E-07	
	5	0.146672620433	4.04399E-14	
0.6	3	0.129471308475		
	4	0.129379000264	9.23082E-05	
	5	0.129378998752	1.51224E-09	
	6	0.129378998752	4.21885E-15	
0.8	3	0.117891261335		
	4	0.111692941017	6.19832E-03	
	5	0.111674669844	1.82712E-05	
	6	0.111674669802	4.22352E-11	
	7	0.111674669802	2.30371E-15	
	0.98	3	0.533358021186	
		4	0.177136522281	3.56221E-01
5		0.101032274269	7.61042E-02	
6		0.096300295595	4.73198E-03	
7		0.096291673251	8.62234E-06	
8		0.096291673243	7.83242E-12	
9	0.096291673243	1.52656E-16		

Table 2: Relative errors for some annuli considered in Figure 7.1. The stopping criterion (6.5) is satisfied with  $k \leq 9$ . As  $\partial B_1^t$  gets closer to  $\partial B_2$  (i.e.,  $t$  increases), we need a bigger truncated matrix to satisfy (6.5) (the same as in two dimensions).



and one can show inductively that

$$\det(M_n) = \frac{1}{\alpha^n} \prod_{k=0}^{n-1} d_k^2 \begin{vmatrix} \cosh \xi_2 & 1 & & & 0 \\ 1 & 2 \cosh \xi_2 & 1 & & \\ & 1 & 2 \cosh \xi_2 & \ddots & \\ & & \ddots & \ddots & 1 \\ 0 & & & 1 & 2 \cosh \xi_2 \end{vmatrix} = \frac{1}{\alpha^n} \left( \prod_{k=0}^{n-1} d_k^2 \right) \cosh(n\xi_2) > 0. \quad (\text{A.2})$$

All the submatrices of  $M_n$  are also  $M_k$  for some  $k$  and, hence, have positive determinant values. Therefore,  $M_n$  is positive definite and  $\sigma_{1,n}^t > 0$  for all  $n \in \mathbb{N}$ .

In the remaining, we prove  $\sigma_{1,n+1}^t < \sigma_{1,n}^t$  by induction on  $n$ . Set

$$p_n(\lambda) := \det(M_n - \lambda I).$$

We note that  $\sigma_{1,n}^t$  is the smallest positive solution to  $p_n(\lambda) = 0$ . From the fact that  $p_n(0) = \det(M_n) > 0$  (see (A.2)) and the intermediate value theorem, it holds that for each  $n$ ,

$$p_n(\sigma_{1,n}^t) = 0, \quad (\text{A.3})$$

$$p_n(\lambda) > 0 \quad \text{for all } 0 < \lambda < \sigma_{1,n}^t. \quad (\text{A.4})$$

In view of (A.1), one can obtain the recursive relation:

$$\begin{aligned} p_2(\lambda) &= \left( \frac{1}{\alpha} 2 \cosh \xi_2 \cdot d_1^2 - \lambda \right) p_1(\lambda) - \frac{1}{\alpha^2} (d_0 d_1)^2, \\ p_{n+2}(\lambda) &= \left( \frac{1}{\alpha} 2 \cosh \xi_2 \cdot d_{n+1}^2 - \lambda \right) p_{n+1}(\lambda) - \frac{1}{\alpha^2} (d_{n+1} d_n)^2 p_n(\lambda) \quad \text{for } n \geq 1. \end{aligned}$$

From (A.3), it then holds that

$$p_2(\sigma_{1,1}^t) = -\frac{1}{\alpha^2} (d_0 d_1)^2 < 0, \quad (\text{A.5})$$

$$p_{n+2}(\sigma_{1,n+1}^t) = -\frac{1}{\alpha^2} (d_{n+1} d_n)^2 p_n(\sigma_{1,n+1}^t) \quad \text{for } n \geq 1. \quad (\text{A.6})$$

From (A.3), (A.4) and (A.5), we have  $\sigma_{1,2}^t < \sigma_{1,1}^t$ . Now, we suppose that  $\sigma_{1,n+1}^t < \sigma_{1,n}^t$  for some  $n \geq 2$ . From (A.4), it follows that  $p_n(\sigma_{1,n+1}^t) > 0$  and, hence,  $p_{n+2}(\sigma_{1,n+1}^t) < 0$  because of (A.6). From (A.3) and (A.4), it then holds that  $\sigma_{1,n+2}^t < \sigma_{1,n+1}^t$ . By induction, we complete the proof.  $\square$

**Proof of Proposition 6.2.** The right inequality is a direct consequence of the variational characterization (2.7) because of the fact that  $u_{1,m}^t \in H_{B_1}^1(B_2) \setminus \{0\}$  for each  $m$ . In the following we prove the left inequality.

We remind the reader that  $P_n L P_n$  is positive definite symmetric matrix on  $H_n$  with respect to the inner product  $(\cdot, \cdot)$  defined by (6.1), which is identical to the finite dimensional positive definite matrix (A.1). Hence, the first eigenvalue  $\sigma_{1,n}^t$  of  $P_n L P_n$  also admits a variational characterization similar to (2.7):

$$\sigma_{1,n}^t = \inf \left\{ \frac{(P_n L P_n v, v)}{(v, v)} : v \in H_n \setminus \{0\} \right\}.$$

By taking  $v = P_n u_1^t$ , we obtain

$$\sigma_{1,n}^t \leq \frac{(P_n L P_n u_1^t, P_n u_1^t)}{(P_n u_1^t, P_n u_1^t)}$$

and

$$\sigma_{1,n}^t - \sigma_1^t \leq \frac{(P_n L P_n u_1^t, P_n u_1^t)}{(P_n u_1^t, P_n u_1^t)} - \sigma_1^t \frac{(P_n u_1^t, P_n u_1^t)}{(P_n u_1^t, P_n u_1^t)} = \frac{(P_n L [P_n u_1^t - u_1^t], P_n u_1^t)}{(P_n u_1^t, P_n u_1^t)}.$$

Now, by using the series expression (4.16) of  $u_1^t$ , we obtain

$$\begin{aligned} & (P_n L (P_n u_1^t - u_1^t), P_n u_1^t) \\ &= - (P_n L [\cos(n\theta)], \cos((n-1)\theta)) \frac{4}{n(n-1)} A_n A_{n-1} \sinh(n(\xi_1 - \xi_2)) \sinh((n-1)(\xi_1 - \xi_2)) \end{aligned}$$

and

$$(P_n u_1^t, P_n u_1^t) = \frac{a_0^2}{w_0^2} \left(1 - \frac{\xi_2}{\xi_1}\right)^2 + \sum_{k=1}^{n-1} \frac{4}{k^2 w_k^2} A_k^2 \sinh^2(k(\xi_1 - \xi_2)) \geq \frac{a_0^2}{w_0^2} \left(1 - \frac{\xi_2}{\xi_1}\right)^2.$$

Hence, it follows that

$$\sigma_{1,n}^t - \sigma_1^t \leq \frac{-\frac{1}{\alpha} \frac{4}{n(n-1)} d_n^2 d_{n-1}^2 A_n A_{n-1} \sinh(n(\xi_1 - \xi_2)) \sinh((n-1)(\xi_1 - \xi_2))}{\frac{a_0^2}{w_0^2} \left(1 - \frac{\xi_2}{\xi_1}\right)^2}. \quad (\text{A.7})$$

We note that the term  $\frac{4}{n(n-1)} d_n^2 d_{n-1}^2$  uniformly bounded independently of  $n$ . From Lemma 4.4 and the proof of Theorem 1.3, we have

$$\lim_{n \rightarrow \infty} \frac{A_n \cosh(n(\xi_1 - \xi_2))}{A_{n-1} \cosh((n-1)(\xi_1 - \xi_2))} = -e^{-\xi_2}.$$

Thus, for big enough  $n_1$ , it holds that

$$|A_n| \cosh(n(\xi_1 - \xi_2)) \leq e^{-\frac{1}{2}n\xi_2} \quad \text{for all } n \geq n_1,$$

which implies

$$-A_n A_{n-1} \sinh(n(\xi_1 - \xi_2)) \sinh((n-1)(\xi_1 - \xi_2)) \leq e^{-n\xi_2}. \quad (\text{A.8})$$

Therefore, the right-hand side of (A.7) tends to 0 as  $n \rightarrow \infty$ . Since the sequence  $\{\sigma_{1,n}^t\}_{n=1}^\infty$  is convergent thanks to Lemma 6.1, we conclude

$$\lim_{n \rightarrow \infty} \sigma_{1,n}^t - \sigma_1^t \leq 0,$$

which completes the proof.  $\square$

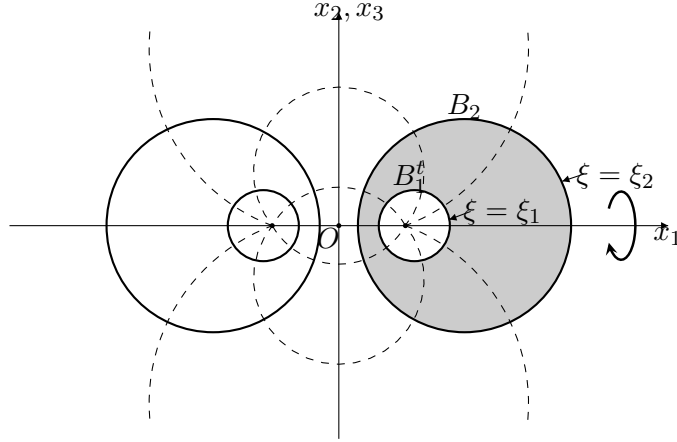


Figure B.1:  $\xi$ -level surfaces (thick) and  $\theta$ -level curves (dashed) of the bispherical coordinate system. The  $\xi$ -level surfaces are simply obtained by rotating the  $\xi$ -level curves in Figure 4.1 with respect to  $x_1$ -axis.

## Appendix B Finite section method in three dimensions

In this section, we introduce the projection method to numerically compute  $\sigma_1^t$  in three dimensions. We rotate the domain in Figure 1.1 with respect to the  $x_1$ -axis and use the bispherical coordinates with which the boundaries of the rotated annulus are coordinate level surfaces.

For  $x = (x_1, x_2, x_3)$  in the Cartesian coordinates, we define bispherical coordinates  $(\xi, \theta, \varphi) \in \mathbb{R} \times [0, \pi] \times [0, 2\pi)$  by

$$(x_1, x_2, x_3) = \left( \frac{\alpha \sinh \xi}{\cosh \xi - \cos \theta}, \frac{\alpha \sin \theta \cos \varphi}{\cosh \xi - \cos \theta}, \frac{\alpha \sin \theta \sin \varphi}{\cosh \xi - \cos \theta} \right),$$

where  $\alpha$  is a positive constant defined as in two dimensions (see (4.6)). We write  $x = x(\xi, \theta, \varphi)$  to indicate its dependence on bispherical coordinates, if necessary. The boundaries of  $B_1^t$  and  $B_2$  are  $\xi$ -level curves of positive values  $\xi_1$  and  $\xi_2$  given by (4.7), respectively. The outward normal derivative on  $\partial B_2$  for a function  $u$  satisfies

$$\frac{\partial u}{\partial \nu} = - \frac{\cosh \xi_2 - \cos \theta}{\alpha} \frac{\partial u}{\partial \xi} \Big|_{\xi=\xi_2}. \quad (\text{B.1})$$

We can expand a harmonic function into separation of variable solutions in bispherical coordinates (see, for example, page 111 in [34]). As the first eigenfunction  $u_1^t$  has the zero trace on  $\partial B_1^t$ , it admits the series representation

$$u_1^t(x(\xi, \theta, \varphi)) = \sqrt{\cosh \xi - \cos \theta} \sum_{n=0}^{\infty} \sum_{m=0}^n \left( e^{(n+\frac{1}{2})\xi} - e^{(n+\frac{1}{2})(2\xi_1-\xi)} \right) P_n^m(\cos \theta) \\ \times \left( D_n^m \cos(m\varphi) + E_n^m \sin(m\varphi) \right) \quad \text{on } B_2 \setminus B_1^t \quad (\text{B.2})$$

for some real coefficients  $D_n^m$  and  $E_n^m$ . Here,  $P_n^m$  denotes the Legendre associated polynomials of order  $m$ . Then, from (B.1) and the definition of the operator  $L$  (see (2.2)), the followings are

also eigenfunctions corresponding to  $\sigma_1^t$  for each  $m \geq 1$ :

$$\sqrt{\cosh \xi - \cos \theta} \left( \sum_{n=m}^{\infty} \left( e^{(n+\frac{1}{2})\xi} - e^{(n+\frac{1}{2})(2\xi_1-\xi)} \right) P_n^m(\cos \theta) D_n^m \right) \cos(m\varphi), \quad (\text{B.3})$$

$$\sqrt{\cosh \xi - \cos \theta} \left( \sum_{n=m}^{\infty} \left( e^{(n+\frac{1}{2})\xi} - e^{(n+\frac{1}{2})(2\xi_1-\xi)} \right) P_n^m(\cos \theta) E_n^m \right) \sin(m\varphi). \quad (\text{B.4})$$

As the functions in (B.3) and (B.4) change sign depending on  $\varphi$  and the first eigenfunction does not change sign (see Lemma 2.1), they are zero functions. We note that  $\{P_n^m(x)\}_{n \geq m}$  is an orthogonal set in  $L^2([-1, 1])$  for each fixed  $m \geq 0$ . In particular,  $\{P_n^m\}_{n \geq m}$  is linearly independent for each fixed  $m \geq 0$ . Hence, it follows that

$$D_n^m = E_n^m = 0 \quad \text{for all } m \neq 0.$$

In other words,

$$u_1^t(x(\xi, \theta, \varphi)) = \sqrt{\cosh \xi - \cos \theta} \sum_{n=0}^{\infty} \left( e^{(n+\frac{1}{2})\xi} - e^{(n+\frac{1}{2})(2\xi_1-\xi)} \right) P_n^0(\cos \theta) D_n^0.$$

On  $\partial B_2$  (i.e.,  $\xi = \xi_2$ ), we have

$$u_1^t(x(\xi_2, \theta, \varphi)) = \sum_{n=0}^{\infty} \tilde{D}_n p_n(\theta),$$

where  $\tilde{D}_n$  are constant coefficients and

$$p_n(\theta) := \sqrt{\cosh \xi_2 - \cos \theta} P_n^0(\cos \theta), \quad n = 0, 1, 2, \dots$$

We observe that for  $n \geq 1$ ,

$$L[p_0] = \frac{1}{2\alpha \sinh\left(\frac{1}{2}(\xi_1 - \xi_2)\right)} \left[ \cosh\left(\frac{1}{2}\xi_1 - \frac{3}{2}\xi_2\right) p_0 - \cosh\left(\frac{1}{2}\xi_1 - \frac{1}{2}\xi_2\right) p_1 \right], \quad (\text{B.5})$$

$$\begin{aligned} L[p_n] &= \frac{\cosh\left(\left(n + \frac{1}{2}\right)\xi_1 - \left(n + \frac{3}{2}\right)\xi_2\right) + 2n \cosh \xi_2 \cosh\left(\left(n + \frac{1}{2}\right)(\xi_1 - \xi_2)\right)}{2\alpha \sinh\left(\left(n + \frac{1}{2}\right)(\xi_1 - \xi_2)\right)} p_n \\ &\quad - \frac{1}{2\alpha \tanh\left(\left(n + \frac{1}{2}\right)(\xi_1 - \xi_2)\right)} [np_{n-1} + (n+1)p_{n+1}]. \end{aligned} \quad (\text{B.6})$$

We set  $Q_n$  be the natural projection onto the space

$$\text{span}\{p_m : 0 \leq m < n\}$$

and denote by  $\sigma_{1,n}^t$  the eigenvalue of the finite section operator  $Q_n L Q_n$ . Here, the finite section operator  $Q_n L Q_n$  is symmetric with respect to the basis  $\left\{ \sqrt{\tanh\left(\left(m + \frac{1}{2}\right)(\xi_1 - \xi_2)\right)} p_m(\theta) \right\}$ . In subsection 6.2, we numerically compute  $\lim_{n \rightarrow \infty} \sigma_{1,n}^t$  for various examples.

## References

- [1] Mikhail Semenovitch Agranovich, *On a mixed Poincaré-Steklov type spectral problem in a Lipschitz domain*, Russ. J. Math. Phys. **13** (2006), 239–244.
- [2] A. R. Aithal and M. H. C. Anisa, *On two functionals connected to the Laplacian in a class of doubly connected domains in space-forms*, Proc. Indian Acad. Sci. Math. Sci. **115** (2005), no. 1, 93–102.
- [3] A. R. Aithal and A. V. Rane, *The first Dirichlet eigenvalue of the Laplacian in a class of doubly connected domains in complex projective space*, Indian J. Pure Appl. Math. **50** (2019), no. 1, 69–81.
- [4] Habib Ammari, Hyeonbae Kang, and Mikyoung Lim, *Gradient estimates for solutions to the conductivity problem*, Math. Ann. **332** (2005), no. 2, 277–286.
- [5] M. H. C. Anisa and R. Mahadevan, *An eigenvalue optimization problem for the  $p$ -Laplacian*, Proc. Roy. Soc. Edinburgh Sect. A **145** (2015), no. 6, 1145–1151.
- [6] M. H. C. Anisa and M. K. Vemuri, *Two functionals connected to the Laplacian in a class of doubly connected domains on rank one symmetric spaces of non-compact type*, Geom. Dedicata **167** (2013), 11–21.
- [7] T. V. Anoop, Vladimir Bobkov, and Sarath Sasi, *On the strict monotonicity of the first eigenvalue of the  $p$ -Laplacian on annuli*, Trans. Amer. Math. Soc. **370** (2018), no. 10, 7181–7199.
- [8] José M. Arrieta, Ángela Jiménez-Casas, and Aníbal Rodríguez-Bernal, *Flux terms and Robin boundary conditions as limit of reactions and potentials concentrating at the boundary*, Rev. Mat. Iberoam. **24** (2008), no. 1, 183–211.
- [9] Rodrigo Bañuelos, Tadeusz Kulczycki, Iosif Polterovich, and Bartłomiej Siudeja, *Eigenvalue inequalities for mixed Steklov problems*, Operator theory and its applications, Amer. Math. Soc. Transl. Ser. 2, vol. 231, Amer. Math. Soc., Providence, RI, 2010, pp. 19–34.
- [10] Catherine Bandle, *Isoperimetric inequalities and applications*, Monographs and Studies in Mathematics, vol. 7, Pitman (Advanced Publishing Program), Boston, Mass.-London, 1980.
- [11] Haim Brezis, *Functional analysis, Sobolev spaces and partial differential equations*, Universitext, Springer, New York, 2011.
- [12] Marc Dambrine, Mohammed El-Djalil Kateb, and Jimmy Lamboley, *An extremal eigenvalue problem for the Wentzell-Laplace operator*, Ann. Inst. H. Poincaré Anal. Non Linéaire **33** (2016), no. 2, 409–450.
- [13] Bodo Dittmar, *Isoperimetric inequalities for the sums of reciprocal eigenvalues*, Progress in partial differential equations, Vol. 1 (Pont-à-Mousson, 1997), Pitman Res. Notes Math. Ser., vol. 383, Longman, Harlow, 1998, pp. 78–87.
- [14] ———, *Eigenvalue problems and conformal mapping*, Handbook of complex analysis: geometric function theory. Vol. 2, Elsevier Sci. B. V., Amsterdam, 2005, pp. 669–686.

- [15] Bodo Dittmar and Reiner Kühnau, *Zur Konstruktion der Eigenfunktionen Stekloffscher Eigenwertaufgaben*, Z. Angew. Math. Phys. **51** (2000), no. 5, 806–819.
- [16] Bodo Dittmar and Alexander Yu Solynin, *The mixed Steklov eigenvalue problem and new extremal properties of the Grötzsch ring*, **115** (2003), 2119–2134.
- [17] Julián Fernández Bonder, Pablo Groisman, and Julio Daniel Rossi, *Optimization of the first Steklov eigenvalue in domains with holes: a shape derivative approach*, Ann. Mat. Pura Appl. (4) **186** (2007), no. 2, 341–358.
- [18] Ailana Fraser and Richard Schoen, *Minimal surfaces and eigenvalue problems*, Geometric analysis, mathematical relativity, and nonlinear partial differential equations, Contemp. Math., vol. 599, Amer. Math. Soc., Providence, RI, 2013, pp. 105–121.
- [19] ———, *Sharp eigenvalue bounds and minimal surfaces in the ball*, Invent. Math. **203** (2016), no. 3, 823–890.
- [20] Ilias Ftouhi, *Where to place a spherical obstacle so as to maximize the first Steklov eigenvalue*, hal-02334941v2.
- [21] Denis S. Grebenkov and Binh T. Nguyen, *Geometrical structure of Laplacian eigenfunctions*, SIAM Rev. **55** (2013), no. 4, 601–667.
- [22] Joseph Hersch and Lawrence E. Payne, *Extremal principles and isoperimetric inequalities for some mixed problems of Stekloff’s type*, Z. Angew. Math. Phys. **19** (1968), 802–817.
- [23] Hyeonbae Kang, Mikyoung Lim, and KiHyun Yun, *Characterization of the electric field concentration between two adjacent spherical perfect conductors*, SIAM J. Appl. Math. **74** (2014), no. 1, 125–146. MR 3162415
- [24] Mikhail Karpukhin, *Maximal metrics for the first Steklov eigenvalue on surfaces*, arXiv:1801.06914.
- [25] Srinivasan Kesavan, *On two functionals connected to the Laplacian in a class of doubly connected domains*, Proc. Roy. Soc. Edinburgh Sect. A **133** (2003), no. 3, 617–624.
- [26] Junbeom Kim and Mikyoung Lim, *Electric field concentration in the presence of an inclusion with eccentric core-shell geometry*, Math. Ann. **373** (2019), no. 1-2, 517–551.
- [27] Tadeusz Kulczycki and Nikolay Kuznetsov, *‘High spots’ theorems for sloshing problems*, Bull. Lond. Math. Soc. **41** (2009), no. 3, 495–505.
- [28] Nikolay Kuznetsov, Tadeusz Kulczycki, Mateusz Kwaśnicki, Alexander Nazarov, Sergey Poborchii, Iosif Polterovich, and Bartłomiej Siudeja, *The legacy of Vladimir Andreevich Steklov*, Notices Amer. Math. Soc. **61** (2014), no. 1, 9–22.
- [29] Marc-Antoine Labrie, *Le théorème spectral pour le problème de Steklov sur un domaine euclidien*, Master’s thesis, Université Laval (2017).
- [30] Pier Domenico Lamberti and Luigi Provenzano, *Viewing the Steklov eigenvalues of the Laplace operator as critical Neumann eigenvalues*, Current trends in analysis and its applications, Trends Math., Birkhäuser/Springer, Cham, 2015, pp. 171–178.

- [31] ———, *Neumann to Steklov eigenvalues: asymptotic and monotonicity results*, Proc. Roy. Soc. Edinburgh Sect. A **147** (2017), no. 2, 429–447.
- [32] Mikyoung Lim and Sanghyeon Yu, *Asymptotics of the solution to the conductivity equation in the presence of adjacent circular inclusions with finite conductivities*, J. Math. Anal. Appl. **421** (2015), no. 1, 131–156. MR 3250470
- [33] Henrik Matthiesen and Romain Petrides, *Monotonicity results for the first Steklov eigenvalue on compact surfaces*, arXiv:1801.08518.
- [34] Parry Moon and Domina Eberle Spencer, *Field theory handbook*, second ed., Springer-Verlag, Berlin, 1988, Including coordinate systems, differential equations and their solutions.
- [35] Jindřich. Nečas, *Direct methods in the theory of elliptic equations*, Springer Monographs in Mathematics, Springer, Heidelberg, 2012.
- [36] Romain Petrides, *Maximizing Steklov eigenvalues on surfaces*, J. Differential Geom. **113** (2019), no. 1, 95–188.
- [37] Alexander G. Ramm and Pappur N. Shivakumar, *Inequalities for the minimal eigenvalue of the Laplacian in an annulus*, Math. Inequal. Appl. **1** (1998), no. 4, 559–563.
- [38] Leoncio Rodriguez-Quiñones, *A critical domain for the first normalized nontrivial steklov eigenvalue among planar annular domains*, arXiv:1909.02121.
- [39] Gopalakrishnan Santhanam and Sheela Verma, *On eigenvalue problems related to the Laplacian in a class of doubly connected domains*, arXiv:1803.05750.
- [40] Francisco-Javier Sayas, Thomas S. Brown, and Matthew E. Hassell, *Variational techniques for elliptic partial differential equations*, CRC Press, Boca Raton, FL, 2019, Theoretical tools and advanced applications.
- [41] D.-H. Seo, *A shape optimization problem for the first mixed Steklov-Dirichlet eigenvalue*, arXiv:1909.06579.
- [42] W. Stekloff, *Sur les problèmes fondamentaux de la physique mathématique (suite et fin)*, Ann. Sci. École Norm. Sup. (3) **19** (1902), 455–490.
- [43] E. Zeidler, *Nonlinear functional analysis and its applications. I*, Springer-Verlag, New York, 1986, Fixed-point theorems, Translated from the German by Peter R. Wadsack.